frontiers | Frontiers in Marine Science

TYPE Original Research
PUBLISHED 14 February 2024
DOI 10.3389/fmars.2024.1329924

OPEN ACCESS

EDITED BY
Hali Kilbourne,
University of Maryland Center for Environmental Science, United States

REVIEWED BY
Logan Brenner,
Columbia University, United States
Allison Lawman,
Colorado College, United States

*CORRESPONDENCE
Mayuri Inoue
inouem@cc.okayama-u.ac.jp

†PRESENT ADDRESSES
Shoko Sakata,
Graduate School of Environmental, Life, Natural Science and Technology, Okayama University, Okayama, Japan
Mayuri Inoue,
Graduate School of Environmental, Life, Natural Science and Technology, Okayama University, Okayama, Japan

‡These authors have contributed equally to this work and share first authorship

RECEIVED 30 October 2023
ACCEPTED 17 January 2024
PUBLISHED 14 February 2024

CITATION
Sakata S, Inoue M, Tanaka Y, Nakamura T, Sakai K, Ikehara M and Suzuki A (2024) Assessment of chemical compositions in coral skeletons (*Acropora digitifera* and *Porites australiensis*) as temperature proxies. *Front. Mar. Sci.* 11:1329924. doi: 10.3389/fmars.2024.1329924

Assessment of chemical compositions in coral skeletons (*Acropora digitifera* and *Porites australiensis*) as temperature proxies

Shoko Sakata[1†‡], Mayuri Inoue[1*†‡], Yasuaki Tanaka[2], Takashi Nakamura[2,3], Kazuhiko Sakai[2], Minoru Ikehara[4] and Atsushi Suzuki[5]

[1]Graduate School of Natural Science and Technology, Okayama University, Okayama, Japan, [2]Sesoko Station, Tropical Biosphere Research Center, University of the Ryukyus, Okinawa, Japan, [3]Faculty of Science, University of the Ryukyus, Okinawa, Japan, [4]Marine Core Research Institute, Kochi University, Nankoku Kochi, Japan, [5]Geological Survey of Japan, National Institute of Advanced Industrial Science and Technology (AIST), Tsukuba, Japan

Although biogenic carbonates, such as foraminifera and coccolithophorids, are valuable tools for reconstructing past environments, scleractinian corals also offer environmental data from tropical to subtropical regions with a higher time resolution. For example, oxygen isotopes ($\delta^{18}O$) and strontium-calcium (Sr/Ca) ratios have been utilized to reconstruct sea surface temperatures and salinity, primarily through the use of massive-type *Porites* sp. from the Pacific, as well as corals like *Diploria* and *Montastrea* from the Atlantic. While a few types of corals other than *Porites* have been utilized in paleoclimate studies, comprehensive evaluations of their geochemical tracers as temperature proxies have not been thoroughly conducted. Therefore, in this study, we focused on branching-type *Acropora*, which are found worldwide and are often present in fossil corals. We conducted a comparison of the chemical compositions ($\delta^{18}O$, $\delta^{13}C$, Sr/Ca, U/Ca, Mg/Ca, and Ba/Ca) of *Acropora digitifera* and *Porites australiensis* through temperature-controlled culture experiments. The validity of using the chemical components of *A. digitifera* as temperature proxies was then evaluated. Three colonies of *A. digitifera* and *P. australiensis* were collected for culture experiments on Sesoko Island, Okinawa, Japan. We reared coral samples in seawater with five different temperature settings (18, 21, 24, 27, 30°). The calcification rate and photosynthesis efficiency (*Fv/Fm*) of each nubbin were measured during the experimental period. After the culture experiment for 77 days, chemical components in skeletal parts grown during the experiment were then measured. Consequently, the mean growth rates and *Fv/Fm* throughout the experiment were higher for *A. digitifera* (0.22%/d and 0.63 for growth rate and *Fv/Fm*) compared to those for *P. australiensis* (0.11%/d and 0.38 for growth rate and *Fv/Fm*). This suggests that the higher efficiency of photosynthesis in *A. digitifera* would promote greater calcification compared to *P. australiensis*. Regarding the potential use as temperature proxies, *A. digitifera* exhibited a strong negative correlation, on average, between $\delta^{18}O$ and the water temperature ($r = 0.95$, $p < 0.001$). The temperature dependency was found to be comparable to that

10.3389/fmars.2024.1329924

reported in *Porites* corals (-0.11 and -0.17 ‰/°C for *P. australiensis* and *A. digitifera*, respectively). Thus, the $\delta^{18}O$ of *A. digitifera* appeared to be a useful temperature proxy, although it was also slightly influenced by skeletal growth rate at the same temperature. A strong negative correlation was also observed between the mean Sr/Ca ratio and temperature in *A. digitifera* ($r = 0.61$, $p < 0.001$) as well as *P. australiensis* ($r = 0.56$, $p < 0.001$), without a clear influence from the skeletal growth rate. Therefore, the skeletal Sr/Ca ratio in corals may have been primarily influenced by water temperature, although large deviations in Sr/Ca were observed in *A. digitifera*, even at the same temperature settings. This deviation can be reduced by subsampling an apical part of a polyp including the axis of skeletal growth. The U/Ca ratio of *A. digitifera* appeared to be affected by internal pH variation within the corals, especially at 30°C. Similar to U/Ca ratios, metabolic and kinetic effects on corals were observed in $\delta^{13}C$ of *A. digitifera* at 18 and 30°C. In addition, considering the variation pattern of both U/Ca and $\delta^{13}C$ of *A. digitifera* at 30°C, it has been suggested that respirations may overwhelm photosynthesis for coral samples at 30°C. Therefore, the U/Ca and $\delta^{13}C$ of *A. digitifera* could potentially be used as proxies of biomineralization processes, whereas the $\delta^{18}O$ and Sr/Ca displayed a high possibility of acting as temperature proxies.

KEYWORDS

coral skeleton, culture experiment, SST proxy, geochemical tracers, calcification mechanism

1 Introduction

The chemical compositions of scleractinian corals, such as $\delta^{18}O$ and Sr/Ca, have been recognized as proxies for sea surface temperature (SST, e.g., Beck et al., 1992; Gagan et al., 2000; Cobb et al., 2003; Ramos et al., 2020). Specifically, massive corals such as *Porites* sp., which are dominated in the Pacific region, have been comprehensively used to reconstruct SST and salinity because they have clear annual bands (D'Olivo et al., 2018; Abram et al., 2020; Goodkin et al., 2021). This reconstruction method has become an indispensable tool in paleoceanography and paleoclimatology. Recently, Sr-U and Li/Mg in coral skeletons have been reported as new proxies for water temperature (Montagna et al., 2014; DeCarlo et al., 2016; Cuny-Guirriec et al., 2019). Although almost all SST records that have contributed to paleoclimate studies have been reconstructed using *Porites* corals, the genus *Isopora*, which belongs to the family Acroporidae, was successfully used in reconstructing SST during the last deglaciation, including the last glacial maximum (Felis et al., 2014). In this previous study, chemical components contained in bulk skeletal samples, rather than sub-samples collected along an annual band, were used to compare SST values. Therefore, it is important to investigate the possibility of using the chemical compositions of genera other than *Porites*, such as *Acropora*, as SST proxies, even though some of these genera grow in a branching morphology. Interestingly, Reynaud et al. (2007) found a temperature dependence of Sr/Ca in *Acropora* sp. based on the culture experiments; however, a potential colony dependence has not been investigated. In this study, we used three colonies of *Acropora digitifera* together with *Porites australiensis* for a temperature-controlled culture experiment to investigate their potential as an SST proxy and any colony dependences on its proxy.

Geochemical proxies in coral skeletons have been used to reconstruct SST as well as salinity, seawater pH, terrestrial runoff, and/or pollution (e.g., Gagan et al., 2000; McCulloch et al., 2003; Pelejero et al., 2005; Inoue et al., 2014; Wei et al., 2015; Genda et al., 2022). However, the detailed mechanisms of incorporation and variability of these proxies occurring within the corals, in addition to their skeletal growth, are not yet fully understood. Although there are studies on the biomineralization of scleractinian corals in terms of their utility as proxies, multiple species other than massive-type *Porites* have been used for this purpose (e.g., Inoue et al., 2007; Gaetani et al., 2011; Inoue et al., 2011; Gagnon et al., 2012; Ram and Erez, 2021). Furthermore, massive *Porites* reportedly show tolerance to environmental stresses, such as high temperature and turbidity, whereas branching *Acropora* seems to be more sensitive to such stresses than massive corals (Loya et al., 2001; Fitt et al., 2009; Jones et al., 2020; Afzal et al., 2023). Loya et al. (2001) reported that massive type colonies, including *Porites* sp., survived the 1998 warming incident in Okinawa, Japan, whereas branched corals, including *A. digitifera*, were heavily impacted. They suggested that this was partially attributable to tissue thickness, in which *Porites* and *Acropora* have thicker and thinner tissues,

respectively. Trophic plasticity is another cause of differences in stress tolerance among genera. Conti-Jerpe et al. (2020) defined coral trophic niches based on $\delta^{13}C$ and $\delta^{15}N$ analyses. They investigated seven genera and found that their trophic levels varied between autotrophs, mixotrophs, and heterotrophs. *Acropora* was clearly categorized as autotrophic, whereas *Porites* was mixotrophic. *Porites* corals generally transmit their symbionts directly from parents to descendants, whereas *Acropora* acquire them anew from the environment in each generation; these processes are referred to as vertical and horizontal transmissions, respectively (Lajeunesse et al., 2004). Thus, the growth strategies of corals and their responses to environmental stresses vary among genera, particularly between the massive *Porites* and the branching *Acropora*. However, direct comparisons of geochemical proxies contained in *Porites* and *Acropora* have not been made. Therefore, it is important to confirm temperature-driven patterns of the incorporation of chemical composition in the coral skeletons of different genera.

In the present study, we performed a culture experiment using both *P. australiensis* and *A. digitifera*, which are predominantly found in the shallow reefs around Okinawa, Japan, within an identical culture system. The study investigated differences in growth patterns and skeletal growth in response to temperature between the two species, as well as their potential as SST proxies. The influence of different growth patterns of two species on the variations of SST proxies is also discussed.

2 Materials and methods

2.1 Preparation of coral sub-samples (nubbins)

Corals (*Porites australiensis* and *Acropora digitifera*) were collected from a fringing reef on Sesoko Island, Okinawa, Japan, on August 12 and October 11, 2013. Three large colonies of each species were collected at intervals of approximately 10 m to avoid sampling of the clones created by fragmentation. The colonies were maintained in a tank containing running seawater from the Sesoko reef under natural light conditions at Sesoko Station, Tropical Biosphere Research Center, University of the Ryukyus, Okinawa, Japan, before the start of the experiment. Similar sized cubes (approximately 2.0 × 2.0 × 2.0 cm) and branches (approximately 2.0-3.0 cm lengths), hereafter referred to as nubbins, were cut from parent colonies of *P. australiensis* and *A. digitifera*, respectively. Prepared nubbins were combined with acrylic plates (3.0 x 3.0 cm and 4.5 x 4.5 cm for *A. digitifera* and *P. australiensis*, respectively) using superglue. Nubbins from each colony of both species were allowed to cure to recover from the stress of cutting in an outdoor aquarium for approximately one month. The skeletal growth rates were measured by buoyant weight method in which coral nubbins were suspended on the balance and underwater weight was measured (Davies, 1989). Because tissue does not contribute to the buoyant weight of the coral when weighed underwater due to its similar density with seawater, only skeletal weight can be directly weighed. For the experiment, six nubbins from each colony of both species were placed in two aquaria at each temperature setting as described in Figure 1. Since weights of all nubbins were measured during the curing period, six nubbins were arranged without significant differences in their initial weight.

2.2 Experimental settings

The seawater of Sesoko reef was filtered through a cartridge-type filter (pore size, 1 μm) and the experiment was performed using a flowthrough system. Duplicate aquaria were filled with filtered seawater adjusted to each temperature setting of 18, 21, 24, 27 and 30˚C. Filled seawater from the duplicate aquaria at each temperature was cooled from the outside by circulating the cooled water in a large tank to maintain the temperature. For seawater of 18 and 21°C, firstly seawater was cooled to approximately 23°C in separate tanks using a chiller, this cooled seawater was then distributed to the experimental aquaria and adjusted the temperature. Furthermore, for the 18°C aquaria, two chillers were externally installed in a large tank to maintain the temperature. The water temperature in each aquarium was recorded every hour using a logger (Thermocron SL, KN Laboratories, Supplementary Figure 1). Because a moderate water flow is necessary to maintain coral health (Nakamura et al., 2005), a filter pump was installed in each tank to generate gentle seawater circulation. Three nubbins from each colony of two species were placed in an aquarium. Therefore, 36 nubbins (six replicates from each colony) were cultured at each temperature with a 12:12 light/dark photoperiod (120-140 mmol/m^2/s) under metal halide lamps (Funnel 2,150 W, Kamihata, Japan). Each aquarium was cleaned by rinsing off with sponges approximately once every two weeks to remove algae attached to it. Using this system, all nubbins were cultured for 77 d, from December 2, 2013, to February 17, 2014.

2.3 Maximum quantum yield of Photosystem II of symbiotic algae

The maximum quantum yields of photosystem II (*Fv/Fm*) of symbiotic algae within all nubbins were measured using a Diving-PAM Underwater Fluorometer (Walz, Germany) after an hour of acclimation to darkness, as described by Iguchi et al. (2012). Because the surface area of the nubbins of *P. australiensis* is wide, measurements were conducted on three randomly selected parts of the colony surface, and the median value was adopted as the representative value of each nubbin. One measurement per nubbin was conducted for branching *A. digitifera*. Measurements were conducted at 14, 45, and 77 d after the start of the experiment in addition to the before the experiment.

2.4 Skeletal growth rate

Coral skeletal weights were measured 14, 35, and 63 d after the start of the experiment as buoyant weight (Davies, 1989; Anthony et al., 2008) in addition to before (day 0) and after (day 77) the

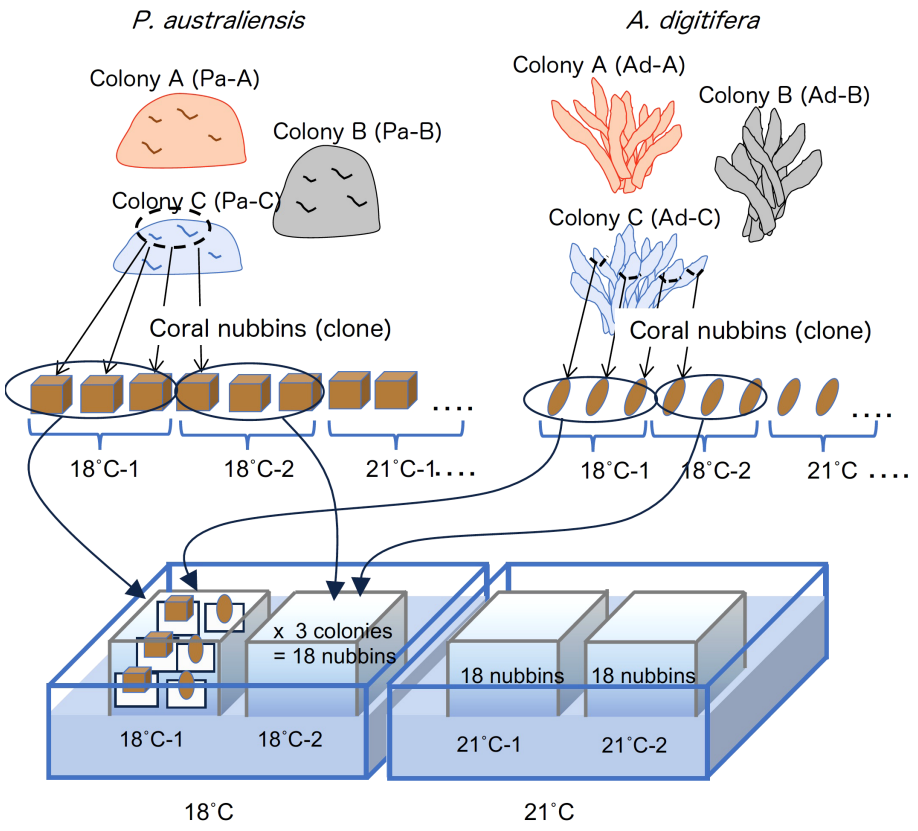

FIGURE 1
Design of the culture experiment conducted in this study.

experiment. The growth rate of coral skeleton during the experiment was calculated as the percentage change in skeletal weight during a specific period in the experiment as below:

$$\text{Growth rate}\,(\%/\text{d}) = \{(W_2 - W_1)/W_1 \times 100\}/\text{Day}$$

where W_1 and W_2 represent the skeletal weight at the beginning and end of a specific period, respectively, and Day is the number of days during the period.

2.5 Collection of skeletal samples

After the experiment was completed, coral nubbins were soaked in an H_2O_2 solution with a pH adjusted to >8 using NaOH for more than 24 h to remove tissue parts. Then, samples were rinsed several times using deionized water and dried in an oven at 40°C. In this study, marking methods, such as using alizarin red, as described by Suzuki et al. (2005), were not used to reduce stress on corals. Therefore, we visually checked the growth area of the skeletons that had grown during the experiment by comparing photographs taken before and after the experiment (Figure 2). Subsequently, the coral skeletons grown in the temperature experiment were scraped off with a spatula and stored in vials. Then collected skeletal parts were gently crushed within vials to make powder samples as bulk sample. Except for the coral samples that apparently died or did not grow large enough to collect powder samples, skeletal samples from almost all nubbins were collected from *A. digitifera*. However, skeletal samples of *P. australiensis* from the 18°C setting could not be collected because their skeletal growth was too small to visually distinguish the skeletal parts that grew during the rearing period.

2.6 Geochemical analyses of skeletal parts grown during the experiment

We measured trace element ratios (Sr/Ca, Mg/Ca, U/Ca, and Ba/Ca ratios) and isotope ratios ($\delta^{13}C$ and $\delta^{18}O$) in skeletal samples grown only during the rearing period using a method similar to that described by Inoue et al. (2018). To measure the concentrations of trace elements, 70 ± 5 μg of skeletal samples was digested in 2% HNO_3 that contained internal standards (^{45}Sc, ^{89}Y, ^{209}Bi) to correct instrumental drift. The concentrations of Sr, Ca, Mg, U, and Ba were measured at Okayama University using an inductively coupled plasma mass spectrometer (ICP-MS; Agilent Technology, 7700x). Standard solutions prepared from JCp-1, a coral (*Porites* spp.) standard material provided by the Geological Survey of Japan (Okai et al., 2002), were measured for every fifth sample for data correction. The relative standard deviations from replicate measurements of the JCp-1 standard were 0.59, 0.81, 1.5 and 3.2% for the Sr/Ca, Mg/Ca, U/Ca, and Ba/Ca ratios, respectively (n = 29). Measurements of $\delta^{18}O$ and $\delta^{13}C$ were conducted using an

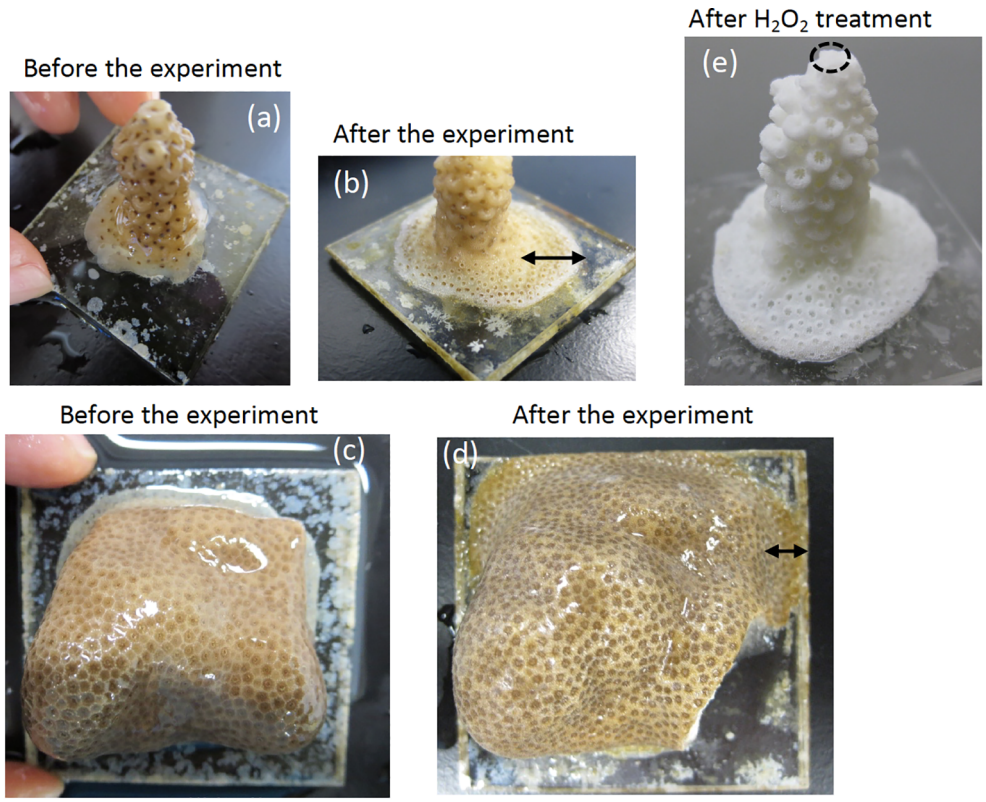

FIGURE 2
Photographs of *A. digitifera* and *P. australiensis* used in this study before **(A, C)** and after the experiment **(B, D)**, respectively. Black arrows in **(B)** and **(D)** represent skeletal parts that grew during the experiment. A photograph of *A. digitifera* following the H_2O_2 treatment to remove organic tissue parts is presented in **(E)**. An approximate place of the tip of *A. digitifera* used for an additional experiment described in the text is circled with dotted line in **(E)**. The sizes of acrylic plates prepared for *A. digitifera* and *P. australiensis* were approximately 3.0 x 3.0 and 4.5 x 4.5 cm, respectively.

online system employing an IsoPrime isotope-ratio mass spectrometer (GV Instruments Ltd.) coupled to a Multicarb automatic sample treatment system at the Center for Advanced Marine Core Research at Kochi University. Approximately 100 ± 10 μg of skeletal samples were used for the measurements and all $\delta^{18}O$ and $\delta^{13}C$ data were normalized to the Vienna Pee Dee Belemnite (V-PDB) scale using the international standard NBS-19 ($\delta^{18}O$ = -2.20‰, $\delta^{13}C$ = -1.95‰) of the National Institute of Standards and Technology. Additionally, the CO-1 ($\delta^{18}O$= -2.4 ‰, $\delta^{13}C$= 2.49 ‰) and IAEA-603 standards ($\delta^{18}O$= -2.73 ‰, $\delta^{13}C$= 2.46 ‰) of the International Atomic Energy Agency were partially used as running standards. The standard deviations for replicate measurements of $\delta^{18}O$ and $\delta^{13}C$ on NBS-19 within the mass spectrometer runs were< 0.1‰ and< 0.05‰ for $\delta^{18}O$ and $\delta^{13}C$, respectively.

2.7 Statistical analysis

The relationship between the chemical compositions of the coral skeleton and water temperature and growth rate were determined using the linear correlation of ordinary least squares. Only for the relations between Sr/Ca and $\delta^{18}O$, that have been generally used as temperature proxies, and water temperature were calibrated by the weighted least square (WLS) method. Growth rate differences among the three colonies were tested via Tukey's pairwise method using PAST (Hammer et al., 2001). Differences of measured chemical compositions between *P. australiensis* and *A. digitifera* were also tested using PAST. In this method, Bayes factor (BF), which quantifies for the hypothesis of unequal means (Hammer et al., 2001), was used to evaluate equal or unequal between two species. Practically, a BF value larger than 3 can be considered as evidence for unequal means. For this test, data at 18˚C were removed since the number of those for *P. australiensis* were very small as mentioned later. In this study, *p*-values below 0.05 were considered statistically significant and correlation coefficients above 0.5 were considered to be correlated unless otherwise noted.

3 Results

3.1 Skeletal growth and maximum quantum yield of Photosystem II of coral nubbins

The skeletal growth rates of the three colonies of *P. australiensis* (Pa-A, Pa-B, and Pa-C) and *A. digitifera* (Ad-A, Ad-B, and Ad-C) during the experiment are shown in Tables 1, 2 and Figure 3. The temporal variability of growth rates throughout the experiment is also presented in Figure 3. For *P. australiensis*, seven and 13

10.3389/fmars.2024.1329924

nubbins from the 18 and 30°C temperature settings appeared dead, respectively, as they were totally bleached and/or covered by algae at the end of the experiment (Table 1). On the other hand, eight nubbins for *A. digitifera* at only 30°C appeared dead (Table 2). Although they appeared dead at the end of the experiment, their skeletal weights were measured up to day 63 that was the last record before the end of the experiment (day 77). Then the growth rate is presented as growth per day (% per day) using weight records up to the period during skeletal growth was observed. Averaged growth rates (%/d) throughout the experiment were 0.11 ± 0.13 and 0.22 ± 0.14%/d which correspond to the skeletal growth of 13.39 ± 16.11 and 3.34 ± 2.83 mg/d, for all nubbins of *P. australiensis* and *A. digitifera*, respectively. Since the initial size and surface area, which affect skeletal growth represented by mg/d, were different between nubbins of *P. australiensis* and *A. digitifera*, hereafter we use growth rate represented by %/d for the comparison and discussion. Then, the mean growth rates were significantly different between two species ($t = 5.35$, $p < 0.001$).

The skeletons of all nubbins, except Pa-B at 30°C, grew during the first 14 out of 77 d of the experiment (Figure 3). Averaged growth rate during the first 2 weeks were higher compared to other periods in both species and 0.19 ± 0.14 and 0.42 ± 0.21%/d were

TABLE 1 Data of each parameter of all nubbins of *P. australiensis* used in the experiment.

Colony Pa-A									
Water temperature (°C)	Sample ID	Growth rate %/day	*Fv/Fm* at the day 45	Mg/Ca mmol/mol	Sr/Ca mmol/mol	Ba/Ca µmol/mol	U/Ca µmol/mol	$\delta^{13}C$ ‰	$\delta^{18}O$ ‰
18	36**	0.036	0.423	–	–	–	–	–	–
	43*	-0.005	0.404	–	–	–	–	–	–
	31*	-0.003	0.219	–	–	–	–	–	–
	40*	-0.002	0.246	–	–	–	–	–	–
	24**	0.000	0.410	–	–	–	–	–	–
	9*	0.037	0.359	–	–	–	–	–	–
21	18	0.082	0.581	5.600	8.793	59.252	1.250	-6.656	-3.927
	15**	0.202	0.565	–	–	–	–	–	–
	2	0.178	0.610	4.530	8.807	70.251	1.311	-6.142	-4.028
	8**	0.122	0.537	–	–	–	–	–	–
	28**	0.144	0.555	–	–	–	–	–	–
	42	0.214	0.498	4.950	8.834	100.856	1.383	-6.484	-3.974
24	17	0.318	0.585	5.485	8.513	31.529	1.184	-6.220	-4.190
	44	0.214	0.570	8.326	8.836	85.974	1.179	–	–
	19	0.260	0.561	5.429	8.772	43.203	1.219	-5.793	-4.039
	34	0.266	0.570	6.148	8.659	36.294	1.244	-6.113	-4.055
	16	0.259	0.579	4.360	8.783	25.535	1.291	-6.629	-5.448
	12	0.195	0.580	4.346	8.772	108.923	1.197	–	–
27	11	0.206	0.460	5.261	8.598	66.015	1.203	-4.142	-4.371
	22	0.112	0.448	7.132	8.753	73.745	1.528	-4.619	-4.307
	6	0.080	0.433	5.680	8.623	57.184	1.273	–	–
	41	0.150	0.471	5.146	8.625	64.254	1.230	–	–
	26	0.152	0.482	4.455	8.672	52.146	1.317	–	–
	25	0.210	0.492	5.444	8.715	52.423	1.453	-3.472	-3.955
30	7	0.079	0.303	5.955	8.393	52.650	1.340	–	–
	39	0.061	0.341	5.083	8.622	26.588	1.218	-5.460	-4.984

(Continued)

10.3389/fmars.2024.1329924

TABLE 1 Continued

Colony Pa-A									
Water temperature (°C)	Sample ID	Growth rate %/day	*Fv/Fm* at the day 45	Mg/Ca mmol/mol	Sr/Ca mmol/mol	Ba/Ca µmol/mol	U/Ca µmol/mol	$\delta^{13}C$ ‰	$\delta^{18}O$ ‰
	29	0.123	0.356	7.345	8.581	98.370	1.381	-5.224	-5.206
	45	0.068	0.350	6.720	–	13.024	1.591	–	–
	3	0.026	0.296	10.360	8.698	17.013	1.423	-3.911	-4.666
	23*	0.080	0.337	–	–	–	–	–	–
Colony Pa-B									
Water temperature (°C)	Sample ID	Growth rate %/day	*Fv/Fm* at the day 45	Mg/Ca mmol/mol	Sr/Ca mmol/mol	Ba/Ca µmol/mol	U/Ca µmol/mol	$\delta^{13}C$ ‰	$\delta^{18}O$ ‰
18	22*	0.037	0.339	–	–	–	–	–	–
	36*	-0.292	0.294	–	–	–	–	–	–
	1**	0.064	0.344	–	–	–	–	–	–
	3**	0.033	0.173	–	–	–	–	–	–
	11**	0.020	0.279	–	–	–	–	–	–
	27**	0.007	0.240	–	–	–	–	–	–
21	21	0.106	0.457	12.453	8.714	82.616	1.377	–	–
	18**	0.131	0.447	–	–	–	–	–	–
	43	0.135	0.436	9.938	9.093	167.242	1.852	-4.264	-3.579
	5**	0.095	0.459	–	–	–	–	–	–
	28	0.133	0.539	7.128	8.914	113.386	1.478	-6.102	-3.965
	39**	0.084	0.485	–	–	–	–	–	–
24	29	0.187	0.506	3.942	8.847	143.304	1.343	-5.518	-4.425
	4**	0.066	0.460	–	–	–	–	–	–
	32	0.164	0.525	4.827	8.718	86.721	1.418	-5.577	-4.335
	45**	0.067	0.482	–	–	–	–	–	–
	42**	0.121	0.407	–	–	–	–	–	–
	25**	0.079	0.379	–	–	–	–	–	–
27	13**	0.042	0.315	–	–	–	–	–	–
	38**	0.021	0.280	–	–	–	–	–	–
	2**	0.031	0.288	–	–	–	–	–	–
	26**	-0.002	0.284	–	–	–	–	–	–
	44**	0.046	0.309	–	–	–	–	–	–
	6**	-0.002	0.261	–	–	–	–	–	–
30	31*	-0.035	0.294	–	–	–	–	–	–
	17*	-0.063	0.155	–	–	–	–	–	–
	8*	-0.028	0.216	–	–	–	–	–	–

(Continued)

10.3389/fmars.2024.1329924

TABLE 1 Continued

Colony Pa-B									
Water temperature (°C)	Sample ID	Growth rate %/day	*Fv/Fm* at the day 45	Mg/Ca mmol/mol	Sr/Ca mmol/mol	Ba/Ca µmol/mol	U/Ca µmol/mol	$\delta^{13}C$ ‰	$\delta^{18}O$ ‰
	20*	-0.086	0.303	–	–	–	–	–	–
	23*	-0.059	0.330	–	–	–	–	–	–
	19*	-0.076	0.408	–	–	–	–	–	–
Colony Pa-C									
Water temperature (°C)	Sample ID	Growth rate %/day	*Fv/Fm* at the day 45	Mg/Ca mmol/mol	Sr/Ca mmol/mol	Ba/Ca µmol/mol	U/Ca µmol/mol	$\delta^{13}C$ ‰	$\delta^{18}O$ ‰
18	24**	-0.047	0.352	–	–	–	–	–	–
	28**	0.042	0.393	–	–	–	–	–	–
	15**	0.047	0.372	–	–	–	–	–	–
	25**	0.041	0.299	–	–	–	–	–	–
	12**	0.021	0.323	–	–	–	–	–	–
	10*	0.049	0.286	–	–	–	–	–	–
21	36	0.334	0.473	6.382	8.992	58.343	1.757	-4.533	-3.801
	16	0.381	0.488	7.762	9.082	–	1.814	-4.416	-3.503
	27	0.301	0.448	8.149	8.989	111.018	1.686	-4.615	-3.883
	19	0.309	0.484	6.349	9.039	86.018	1.727	-4.879	-3.454
	13	0.368	0.469	4.558	8.775	36.766	1.681	-5.009	-4.335
	14**	0.383	0.484	–	–	–	–	–	–
24	4	0.274	0.403	3.816	8.936	63.119	1.224	-5.709	-4.134
	2	0.311	0.386	5.313	8.412	40.542	1.130	-6.136	-4.412
	17	0.379	0.426	8.768	8.628	109.407	1.430	-4.321	-3.914
	21	0.304	0.387	13.312	8.401	104.554	1.552	-3.613	-4.113
	30	0.316	0.383	3.827	8.704	103.494	1.313	-4.450	-4.559
	39	0.308	0.375	5.203	8.768	100.186	1.586	-3.900	-4.222
27	5**	0.119	0.286	–	–	–	–	–	–
	11**	0.140	0.262	–	–	–	–	–	–
	18	0.166	0.258	8.586	8.915	118.189	1.545	-3.287	-4.473
	6**	0.155	0.278	–	–	–	–	–	–
	34	0.172	0.250	11.463	8.559	58.051	1.537	–	–
	33	0.181	0.248	7.926	8.773	55.581	1.534	-3.347	-4.300
30	1*	0.013	0.204	–	–	–	–	–	–
	20*	0.025	0.191	–	–	–	–	–	–
	37*	-0.004	0.197	9.565	8.460	88.587	1.782	-3.839	-5.047
	3*	-0.044	0.220	5.984	8.934	33.560	1.474	-4.716	-4.401

(Continued)

10.3389/fmars.2024.1329924

TABLE 1 Continued

Colony Pa-C									
Water temperature (°C)	Sample ID	Growth rate %/day	*Fv/Fm* at the day 45	Mg/Ca mmol/mol	Sr/Ca mmol/mol	Ba/Ca μmol/mol	U/Ca μmol/mol	$\delta^{13}C$ ‰	$\delta^{18}O$ ‰
	32*	0.070	0.340	6.798	8.290	76.510	–	–	–
	8*	0.005	0.279	–	–	–	–	–	–

Sample IDs with * indicate that the nubbin appeared to be dead after the experiment, and those with ** indicate that an insufficient amount of bulk skeletal samples were collected.

TABLE 2 Data of each parameter of all nubbins of *A. digitifera* used in the experiment.

Colony Ad-A									
Water temperature (°C)	Sample ID	Growth rate %/day	*Fv/Fm* at the day 45	Mg/Ca mmol/mol	Sr/Ca mmol/mol	Ba/Ca μmol/mol	U/Ca μmol/mol	$\delta^{13}C$ ‰	$\delta^{18}O$ ‰
18	16	0.016	0.574	6.821	8.997	8.878	1.533	-0.993	-2.416
	26	0.004	0.573	4.924	9.010	11.898	1.901	-0.041	-2.036
	44	-0.080	0.544	–	8.540	–	1.370	0.820	-1.990
	10**	0.002	0.419	–	–	–	–	–	–
	11	0.003	0.412	5.357	9.115	18.319	1.809	0.307	-2.121
	8	0.004	0.507	4.990	8.950	10.739	1.842	-0.296	-2.554
21	1	0.192	0.681	7.623	8.986	17.101	1.557	-2.360	-2.788
	24	0.191	0.659	5.021	9.040	15.733	1.627	-3.018	-2.996
	35	0.254	0.673	–	8.525	15.042	1.466	-2.295	-2.920
	29	0.269	0.677	7.434	8.939	15.424	1.337	-3.198	-3.063
	32	0.228	0.600	4.409	9.109	13.582	1.761	-1.651	-2.643
	5	0.280	0.674	9.351	8.956	10.874	1.609	-2.429	-2.846
24	27**	0.215	0.722	–	–	–	–	–	–
	23	0.064	0.609	6.464	8.807	7.288	1.721	-1.879	-3.330
	36	0.327	0.675	11.416	8.555	7.532	1.369	-1.546	-3.189
	43	0.341	0.700	4.684	8.941	9.480	1.530	-1.662	-3.335
	18	0.278	0.689	11.373	8.692	10.475	1.397	-1.345	-3.356
	38	0.426	0.647	–	–	12.159	1.425	-0.871	-3.020
27	37	0.149	0.665	6.133	8.822	6.382	1.505	-1.280	-3.356
	31	0.265	0.682	7.226	8.673	10.087	1.422	-0.306	-3.321
	34	0.373	0.684	11.655	8.481	17.550	1.396	-0.543	-3.708
	20	0.149	0.674	5.210	8.831	10.931	1.488	-1.106	-3.772
	39	0.183	0.687	6.166	8.809	5.697	1.685	-0.689	-3.647
	45	0.390	0.679	11.805	8.529	15.676	1.511	-1.299	-3.727
30	28*	0.168	0.644	5.481	8.855	8.399	1.695	-3.050	-4.393
	41*	0.201	0.670	5.039	8.837	9.285	1.764	-3.211	-4.608

(Continued)

10.3389/fmars.2024.1329924

TABLE 2 Continued

Colony Ad-A									
Water temperature (°C)	Sample ID	Growth rate %/day	*Fv/Fm* at the day 45	Mg/Ca mmol/mol	Sr/Ca mmol/mol	Ba/Ca µmol/mol	U/Ca µmol/mol	$\delta^{13}C$ ‰	$\delta^{18}O$ ‰
	21	0.104	0.655	7.696	8.601	6.551	1.504	-3.612	-4.506
	9	0.116	0.651	5.033	8.967	7.733	1.672	-3.063	-4.272
	17*	0.264	0.689	9.151	8.607	8.710	1.514	-2.458	-4.064
	14	0.174	0.685	6.973	8.627	5.805	1.680	-2.511	-4.190
Colony Ad-B									
Water temperature (°C)	Sample ID	Growth rate %/day	*Fv/Fm* at the day 45	Mg/Ca mmol/mol	Sr/Ca mmol/mol	Ba/Ca µmol/mol	U/Ca µmol/mol	$\delta^{13}C$ ‰	$\delta^{18}O$ ‰
18	13	0.060	0.454	6.990	9.153	10.585	1.984	-0.913	-2.367
	42	0.069	0.594	5.563	9.293	–	1.864	–	-2.661
	27	0.064	0.479	11.453	8.815	21.349	1.793	-1.129	-2.736
	4	0.036	0.419	8.430	9.036	16.973	1.830	-0.706	-2.160
	1	0.041	0.494	5.841	9.271	28.527	1.882	-1.040	-2.429
	23	0.036	0.454	5.210	9.155	11.584	1.817	-0.844	-2.605
21	20	0.391	0.604	4.506	9.080	16.541	1.500	-3.582	-3.197
	3	0.406	0.642	7.518	9.007	16.270	1.529	-3.920	-3.169
	38	0.362	0.625	5.063	9.124	16.842	1.495	-3.631	-3.075
	41	0.154	0.649	5.304	9.145	23.336	1.630	-2.648	-2.929
	15	0.120	0.648	4.593	9.205	19.434	1.900	-1.679	-2.719
	25	0.174	0.640		8.564	16.318	1.741	-1.313	-2.155
24	10	0.292	0.592	–	8.456	12.610	1.375	-1.958	-3.011
	45	0.473	0.642	4.981	9.008	10.117	1.493	-2.405	-3.451
	19	0.347	0.628	4.734	9.018	13.338	1.522	-2.301	-3.400
	14	0.262	0.616	–	8.768	–	1.357	-3.051	-3.482
	12	0.190	0.649	6.469	9.006	14.345	1.634	-2.348	-3.149
	43	0.311	0.633	6.858	8.961	12.232	1.371	-3.005	-3.478
27	11	0.353	0.595	5.495	8.833	10.662	1.432	-1.630	-3.891
	31	0.276	0.611	9.595	8.636	14.309	1.326	-1.925	-4.027
	7	0.374	0.612	8.572	8.757	7.997	1.357	–	–
	35	0.119	0.649	6.120	8.921	9.273	1.732	-1.276	-3.630
	2	0.445	0.621	7.988	8.757	11.915	1.330	-2.501	-4.238
	22	0.317	0.606	5.485	8.826	13.910	1.313	-2.204	-3.868
30	36	0.187	0.628	6.775	8.793	6.308	1.452	-3.979	-4.656
	44*	-0.018	0.562	8.127	8.700	8.728	1.806	-2.854	-4.214
	29	0.185	0.677	9.568	8.562	14.845	1.433	-3.108	-4.549

(Continued)

10.3389/fmars.2024.1329924

TABLE 2 Continued

Colony Ad-B									
Water temperature (°C)	Sample ID	Growth rate %/day	*Fv/Fm* at the day 45	Mg/Ca mmol/mol	Sr/Ca mmol/mol	Ba/Ca µmol/mol	U/Ca µmol/mol	$\delta^{13}C$ ‰	$\delta^{18}O$ ‰
	39*	0.112	0.592	5.500	8.813	5.226	1.710	-2.524	-4.294
	16*	0.109	0.674	7.648	8.741	7.422	1.574	-3.285	-4.341
	26*	0.096	0.643	–	8.436	11.578	1.463	-2.222	-3.964
Colony Ad-C									
Water temperature (°C)	Sample ID	Growth rate %/day	*Fv/Fm* at the day 45	Mg/Ca mmol/mol	Sr/Ca mmol/mol	Ba/Ca µmol/mol	U/Ca µmol/mol	$\delta^{13}C$ ‰	$\delta^{18}O$ ‰
18	43	0.054	0.600	3.993	9.271	11.616	1.720	-1.606	-2.007
	13	0.077	0.496	4.003	9.296	11.051	1.719	-1.025	-2.174
	36	0.074	0.515	6.744	9.140	9.623	1.930	-0.747	-1.725
	20	0.021	0.480	4.276	9.196	12.300	1.991	-0.487	-1.728
	39	0.043	0.452	4.879	9.271	15.450	2.057	-1.525	-2.045
	26	0.046	0.434	–	8.607	20.261	1.549	-0.563	-2.320
21	27	0.260	0.686	4.309	9.170	12.877	1.410	-3.293	-3.196
	17	0.380	0.665	6.204	9.044	14.213	1.367	-2.762	-3.022
	37	0.341	0.676	5.240	8.983	10.716	–	-3.689	-3.247
	12	0.482	0.665	6.192	8.916	17.203	1.265	-3.327	-3.156
	7	0.274	0.685	5.743	9.089	12.927	1.571	-2.170	-2.516
	41	0.300	0.650	4.444	9.110	–	1.403	-2.553	-2.842
24	16	0.294	0.698	7.403	8.805	8.270	1.262	-1.971	-3.355
	8	0.242	0.692	6.517	8.763	8.447	1.371	-1.786	-3.349
	6	0.405	0.690	5.909	8.784	8.246	1.384	-2.200	-3.476
	1	0.349	0.701	4.868	8.902	10.122	1.421	-1.691	-3.490
	18	0.460	0.692	12.363	8.434	11.146	1.371	-1.783	-3.424
	38	0.302	0.695	5.533	8.927	8.761	1.384	-1.919	-3.283
27	10	0.258	0.683	12.265	8.685	8.664	1.317	-1.166	-4.276
	28	0.365	0.707	5.839	8.815	11.048	1.229	-0.749	-3.794
	14	0.276	0.701	4.907	8.861	8.076	1.349	-1.025	-3.978
	11	0.350	0.699	5.835	8.796	10.644	1.491	-1.828	-4.104
	5	0.469	0.666	7.045	8.730	7.609	1.303	-2.557	-4.438
	23	0.411	0.697	5.412	8.822	11.468	1.290	-2.240	-4.062
30	45	0.156	0.705	10.913	8.580	15.214	1.504	-3.588	-4.784
	32*	0.216	0.693	6.766	8.631	7.908	1.515	-3.648	-4.732
	29	0.210	0.687	4.907	8.808	4.853	1.512	-2.975	-4.380
	34	0.170	0.680	4.932	8.711	6.102	1.595	-3.250	-4.554

(Continued)

10.3389/fmars.2024.1329924

TABLE 2 Continued

Colony Ad-C									
Water temperature (°C)	Sample ID	Growth rate %/day	*Fv/Fm* at the day 45	Mg/Ca mmol/mol	Sr/Ca mmol/mol	Ba/Ca µmol/mol	U/Ca µmol/mol	$\delta^{13}C$ ‰	$\delta^{18}O$ ‰
	35	0.146	0.711	5.063	8.788	8.338	1.406	-3.160	-4.282
	9	0.151	0.701	7.048	8.783	13.826	1.535	-2.508	-4.115

Sample IDs with * indicate that the nubbin appeared to be dead after the experiment, and those with ** indicate that an insufficient amount of bulk skeletal samples were collected.

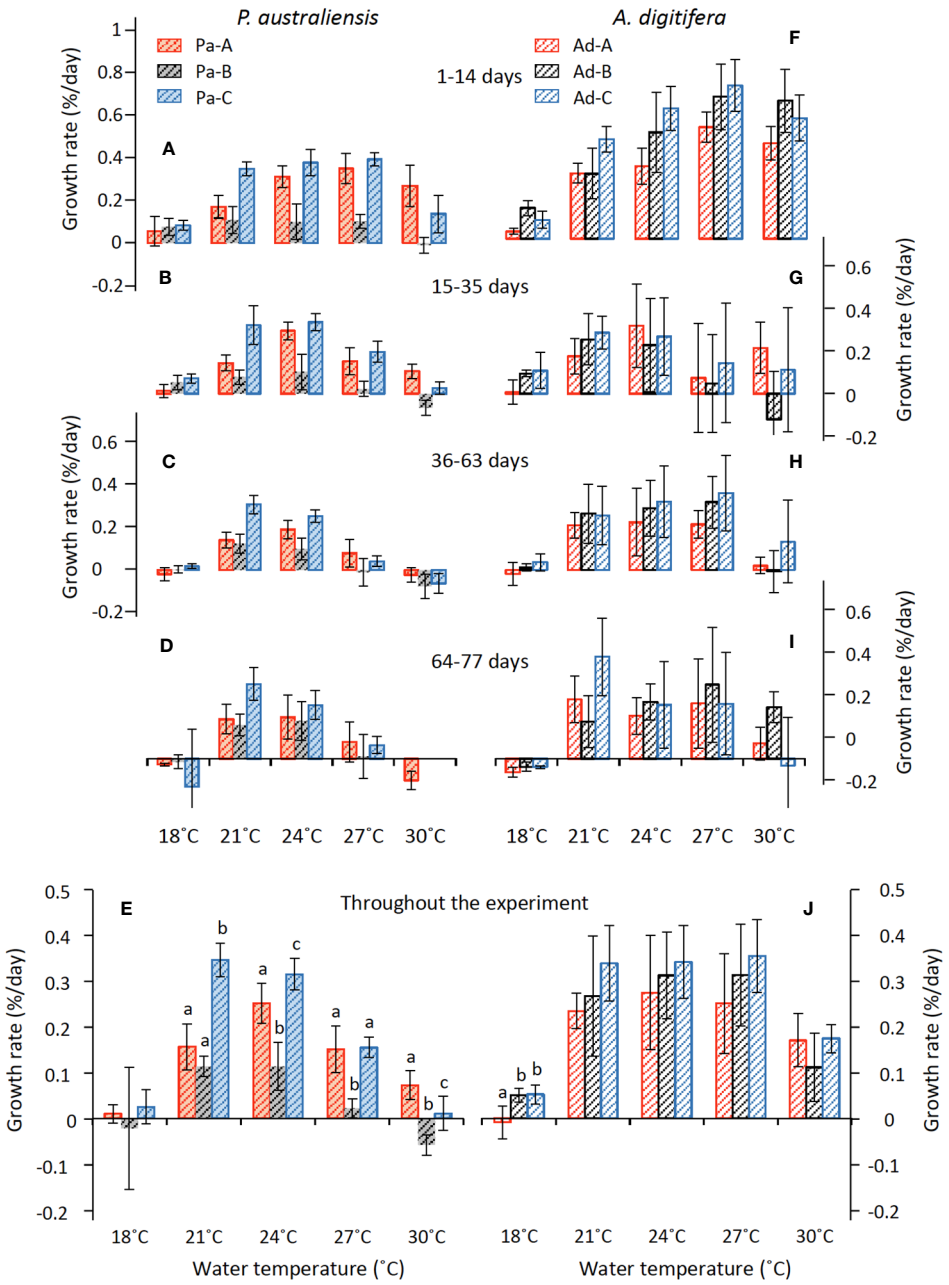

FIGURE 3
Variations in growth rate (mean ± 1sd) of *P. australiensis* **(A–E)** and *A. digitifera* **(F–J)** as a function of water temperature during the culture experiment for 77 d. The various colors indicate each colony; red, black and blue represent colonies A, B and C, respectively. Different letters (a, b, c) described on the bar indicates significant differences ($p < 0.05$) between the colonies at the same temperature. There are no colony differences in growth rate of *P. australiensis* at 18°C and *A. digitifera* from 21 to 30°C.

observed for *P. australiensis* and *A. digitifera* (Figures 3A, F). Temporal changes of mean growth rate for *P. australiensis* and *A. digitifera* for the three periods (15-35, 36-63, and 64-77 days) after the first two weeks were 0.12, 0.07, and 0.08 and 0.15, 0.18, and 0.15%/d, respectively. Deviations in the growth rate of each colony of *A. digitifera* were greater than that of *P. australiensis* throughout the experiment and at all temperature settings. Excepting the 18°C temperature, significant colony differences in the final growth rates throughout the experiment were observed for *P. australiensis*, whereas no differences were recorded for *A. digitifera* (Figures 3E, J).

Responses of the maximum photosynthetic quantum yield (*Fv*/*Fm*) against temperature were significantly higher in *A. digitifera* (0.63 ± 0.08) compared to those of *P. australiensis* throughout the experiment (0.38 ± 0.11; $t = 16.66$, $p < 0.001$; Figure 4). Temporal changes of mean *Fv*/*Fm* of *P. australiensis* and *A. digitifera* at each four measurements (before, the day 14, 45, and the end of the experiment) were 0.49, 0.42, 0.38, and 0.42 and 0.69, 0.67, 0.63, and 0.61, respectively. The values of *Fv*/*Fm* were almost the same for all three colonies of *A. digitifera*, with small deviations throughout the experiment (Figures 4E–H). In contrast, the *Fv*/*Fm* of Pa-A was higher than those of the other two colonies for *P. australiensis*, especially during the first half of the experiment (Figures 4A, B).

Because both the growth rates and *Fv*/*Fm* decreased and several nubbins were apparently dead in the last two weeks, we compared the relationships between the skeletal growth and *Fv*/*Fm* using data from days 63 and 45 for the growth rate and *Fv*/*Fm*, respectively. Consequently, strong positive relationships ($0.74 < r < 0.87$, $p < 0.001$) were observed in all three colonies of *P. australiensis*, whereas moderate to weak correlations ($0.37 < r < 0.56$, $p < 0.04$) were recorded for *A. digitifera* (Figure 5). This relation was maintained when data at 18°C was removed for *P. australiensis*, whereas it collapsed for *A. digitifera*. This suggests that the weak to moderate relationships found in *A. digitifera* were generated predominantly by data at 18°C in which *Fv*/*Fm* was lower (Figure 4G), rather than the trend found in all temperature settings.

3.2 Variations of chemical compositions

Regarding the measurements of chemical compositions, several nubbins could not be analyzed owing to an exceedingly small growth rate during the experiment, especially for the nubbins of *P. australiensis* grown under 18°C. In addition, we could not collect enough skeletal powder (> 70 and > 100 μg for trace elements and isotope measurements, respectively) from another several samples due to difficulties to distinguish the newly grown skeletal parts. On the other hand, even in nubbins that appeared to be dead at the end of the experiment, chemical compositions could be measured if they had grown sufficiently before growth stopped. Furthermore, data that were outliers based on the box plots of each Me/Ca were omitted. Therefore, the number of data obtained from each colony varied (Tables 1, 2). Correlations between each chemical composition within each species were presented in Table 3. No consistent and significant relationships were found in correlations ($r > 0.5$) between geochemical tracers for both species. However, a strong positive correlation ($r = 0.74$, $p < 0.001$) was found between Sr/Ca and $\delta^{18}O$ for *A. digitifera* although that for *P. australiensis* was moderate and not significant ($r = 0.48$, $p = 0.06$). The relationships between water temperature, growth rate, and chemical composition are shown in Figures 6, 7, and Supplementary Figure 2.

3.2.1 $\delta^{18}O$

The mean $\delta^{18}O$ of *P. australiensis* and *A. digitifera* were -4.25 ± 0.46 and -3.63 ± 0.61 ‰ (mean ± 1sd), respectively. A Bayes factor (BF) between two dataset (*A. digitifera* and *P. australiensis*) was > 100 which indicates that there is a significant difference between them. There were no colony differences in $\delta^{18}O$ within the same species (Supplementary Table 1). Since significant correlations were found between water temperature and $\delta^{18}O$ of *P. australiensis* ($r = 0.67$, $p = 0.001$) and *A. digitifera* ($r = 0.95$, $p < 0.001$, Figure 6A), calibrations were established based on the WLS method as below. We used $1/\sigma^2$ as the weight where σ is standard deviations of water temperature at each temperature setting throughout the whole period of experiments (Supplementary Figure 1).

$$P.\ australiensis: \delta^{18}O = -0.11(\pm 0.002)\,T - 1.51(\pm 0.04),\ \text{RMSR } 0.03°C\ (n = 32)$$

$$A.\ digitifera: \delta^{18}O = -0.17(\pm 0.001)\,T + 0.87(\pm 0.02),\ \text{RMSR } 0.02°C\ (n = 87)$$

where T is water temperature. On the other hand, $\delta^{18}O$ in both species showed no significant relationship against the growth rate (Figures 7A, G).

3.2.2 Sr/Ca

The mean Sr/Ca of *P. australiensis* and *A. digitifera* were 8.73 ± 0.19 and 8.82 ± 0.19 mmol/mol, respectively. A BF between two dataset was 2.15 which indicates no evidence for either equal or unequal. There were no colony differences in Sr/Ca within the same species (Supplementary Table 1). Since significant correlations were also found between water temperature and Sr/Ca of *P. australiensis* ($r = 0.56$, $p < 0.001$) and *A. difitifera* ($r = 0.61$, $p < 0.001$. Figure 6B), calibrations based on the WLS were established as below.

$$P.\ australiensis: \mathrm{Sr/Ca} = -0.040(\pm 0.001)\,T + 9.75(\pm 0.017),\ \text{RMSR } 0.01°C\ (n = 41)$$

$$A.\ digitifera: \mathrm{Sr/Ca} = -0.033(\pm 0.0005)\,T + 9.68(\pm 0.011),\ \text{RMSR } 0.02°C\ (n = 87)$$

where T is water temperature. Same as $\delta^{18}O$, Sr/Ca in both species showed no significant relationship against the growth rate (Figures 7B, H).

3.2.3 U/Ca

The mean U/Ca of *P. australiensis* and *A. digitifera* were 1.43 ± 0.20 and 1.49 ± 0.15 μmol/mol, respectively. A BF between two

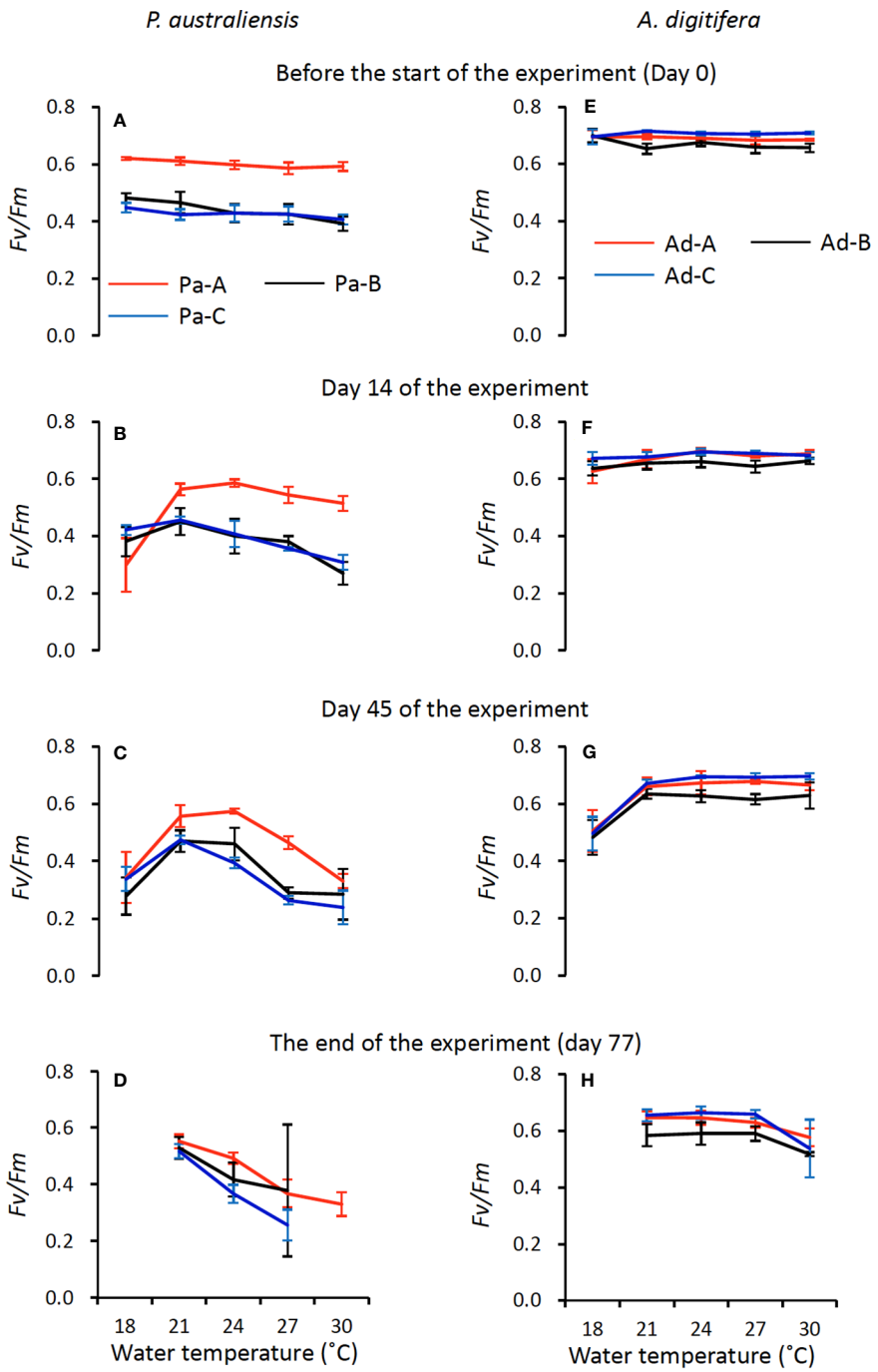

FIGURE 4
Temporal variations of maximum quantum yield of Photosystem II (*Fv/Fm*) of symbiotic algae (mean ± 1sd) in *P. australiensis* **(A-D)** and *A. digitifera* **(E-H)** as a function of water temperature.

dataset was 1.98 which indicates no evidence for either equal or unequal. Although a difference between Pa-A and Pa-C was found, no clear and consistent colony differences were found for other colonies of both species (Supplementary Table 1). Moderate correlations were found between U/Ca and water temperature for only Ad-B ($r = 0.56$, $p < 0.001$) and Ad-C ($r = 0.50$, $p < 0.001$; Supplementary Figure 2K). However no consistent relationships were observed for other colonies and non-linear relations were found in mean U/Ca as a function of water temperature as seen in Figure 6E. In contrast, significant negative correlations between U/Ca and the growth rate were found in two colonies (Ad-B and Ad-C) and all colonies combined for *A. digitifera* (Figure 7K).

3.2.4 $\delta^{13}C$

The mean $\delta^{13}C$ of *P. australiensis* and *A. digitifera* were -4.97 ± 1.03 and -2.32 ± 0.89 ‰, respectively. A BF between two dataset was > 100, indicating a significant difference between them. Similar with U/Ca, although a difference between Pa-A and Pa-C was found, no

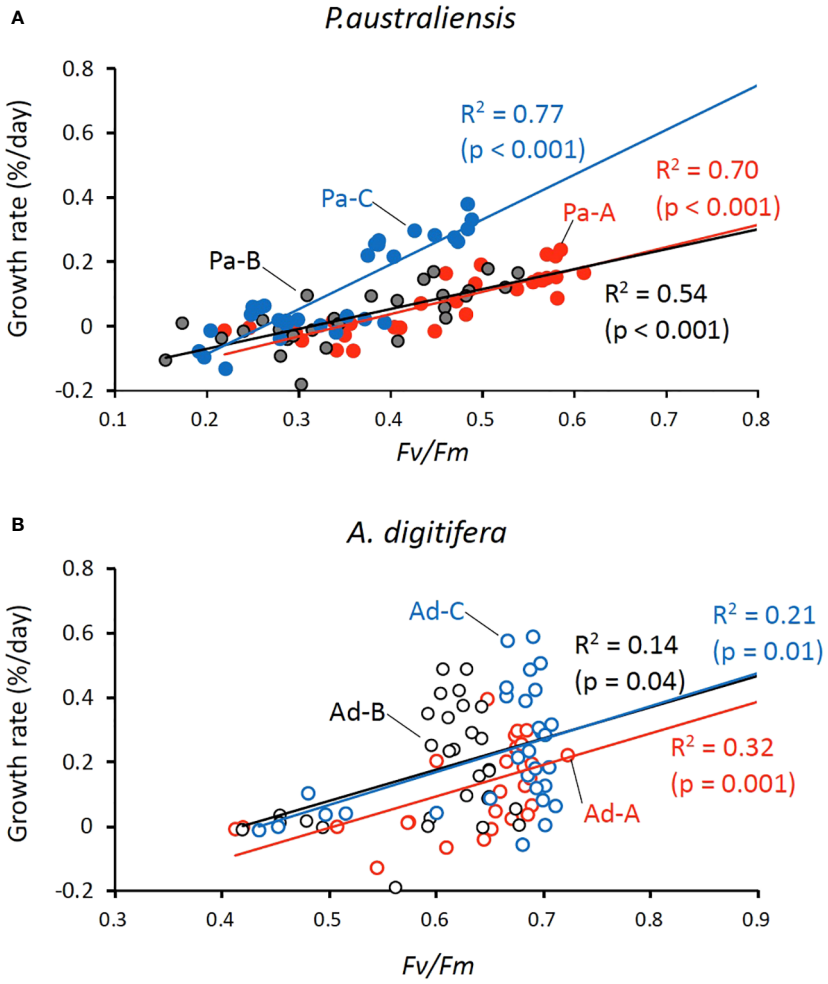

FIGURE 5
Relationships between the skeletal growth rate and *Fv/Fm* for *P. australiensis* **(A)** and *A. digitifera* **(B)** Because several coral nubbins appeared dead within the final 2 weeks of the experiment, growth rates were calculated for 63 d instead of overall period (77 d) of the experiment; values of *Fv/Fm* correspond to those at day 45 of the experiment. Note that the scale of *Fv/Fm* differs between the panel **A** and **B**.

clear and consistent colony differences were found for other colonies of both species (Supplementary Table 1). In addition, no significant correlations were found in both growth rate and water temperature and $\delta^{13}C$ of both species (Figures 6D, 7D, J).

3.2.5 Mg/Ca

The mean Mg/Ca of *P. australiensis* and *A. digitifera* were 6.66 ± 2.33 and 6.79 ± 2.16 mmol/mol, respectively. A BF between two dataset was 0.22 which indicates that there is no difference between

TABLE 3 Correlation coefficients between each chemical compositions.

	Mg/Ca	Sr/Ca	Ba/Ca	U/Ca	$\delta^{13}C$	$\delta^{18}O$	
Mg/Ca		-0.16	0.29	**0.51**	**0.57**	0.09	Mg/Ca
Sr/Ca	-0.67		0.31	0.43	-0.02	0.48	Sr/Ca
Ba/Ca	0.07	0.4		0.45	0.26	0.3	Ba/Ca
U/Ca	-0.28	**0.54**	0.19		0.58	0.28	U/Ca
$\delta^{13}C$	0.04	0.18	0.09	0.34		0.03	$\delta^{13}C$
$\delta^{18}O$	-0.23	**0.74**	0.45	**0.53**	**0.57**		$\delta^{18}O$

Blue and red numbers indicate the correlation coefficients between the chemical compositions *P. australiansis* and *A. digitifera*, respectively. Significant correlations are indicated by bold numbers ($p<0.05$).

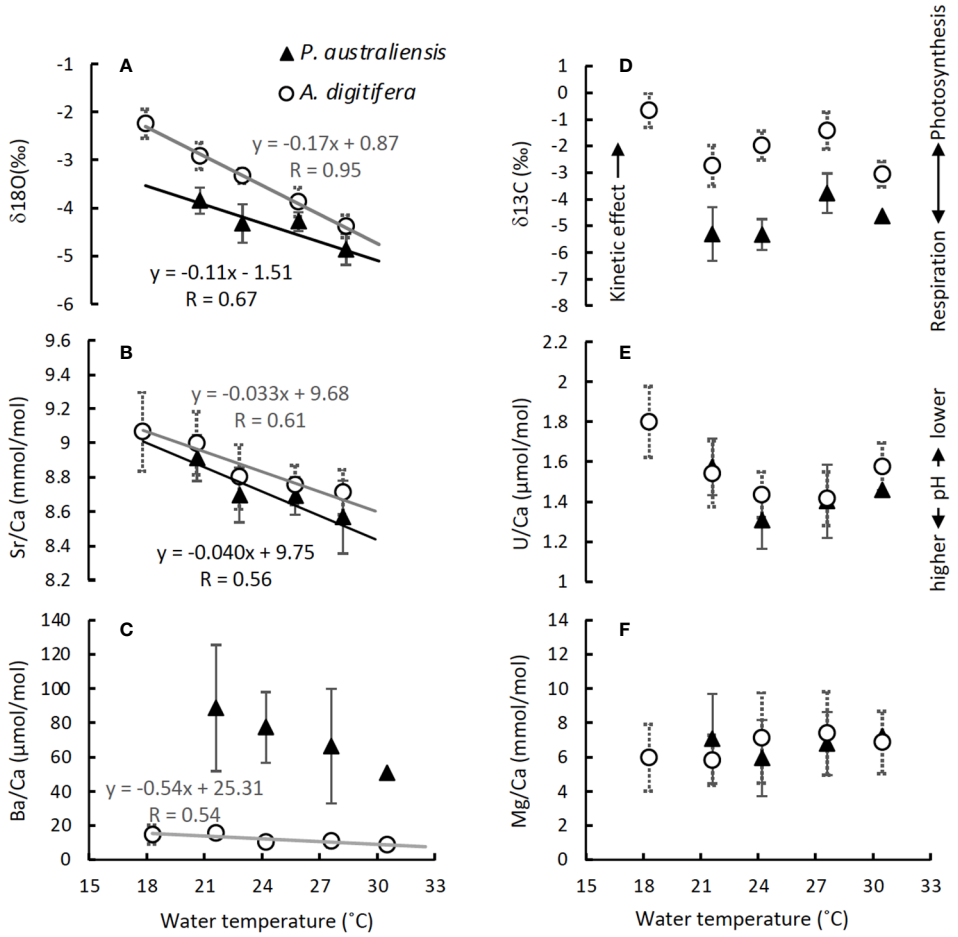

FIGURE 6
Variations in δ18O **(A)**, Sr/Ca **(B)**, Ba/Ca **(C)**, δ13C **(D)**, U/Ca **(E)** and Mg/Ca **(F)** of each colony of *P. australiensis* and *A. digitifera* as a function of water temperature. Data are presented as mean ± 1sd of all data measured on three colonies, but calibrations are performed using all individual data as seen in Supplementary Figure 2. Calibrations are presented only for those with an observed significant relationship ($r > 0.5$, $p < 0.05$).

them. In addition, there were no colony differences in both species (Supplementary Table 1). Although only one colony (Ad-A) showed a positive correlation between Mg/Ca and the growth rate (Figure 7L), no consistent correlations were found in both growth rate and water temperature and Mg/Ca of both species (Figures 6F, 7F, L).

3.2.6 Ba/Ca

Variations of Ba/Ca were very large and the mean Ba/Ca of *P. australiensis* and *A. digitifera* were 72.50 ± 34.72 and 11.27 ± 3.86 μmol/mol, respectively. Obviously, there is a difference of Ba/Ca between two species with a BF >100. Colony differences were found between Pa-A and Pa-B and Pa-B and Pa-C in addition to Ad-B and Ad-C (Supplementary Table 1). Although no correlations between Ba/Ca and growth rate were found for both species, a negative correlation was found between water temperature and mean Ba/Ca for *A. digitifera* (Figures 6C, 7C, I). In contrast to *A. digitifera*, Ba/Ca of three colonies of *P. australiensis* varies largely and showed no temperature dependences.

4 Discussion

4.1 Growth patterns of *P. australiensis* and *A. digitifera* in response to water temperature and the *Fv/Fm*

Skeletal growth rates of *P. australiensis* during the culture experiment were mostly higher (> 0.1%/d) at 24°C and lower at 18 and 30˚C (< 0.1%/d) with significant colony differences (Figure 3). Similarly, those of *A. digitifera* were higher at 21-27°C and lower at 18 and 30°C, but there were no colony differences in the skeletal growth rate at each temperature except for 18°C (Figure 3J). However, deviations in the growth rate of each colony of *P. australiensis* were small, but large for *A. digitifera*. Therefore, growth patterns, including growth variations among colonies and within a colony, differed between the two species. In addition, the average growth rate for 21-27°C of *A. digitifera* (0.30 ± 0.10%/day) was significantly higher than that of *P. australiensis* (0.18 ± 0.11%/day) which is mostly consistent to findings observed

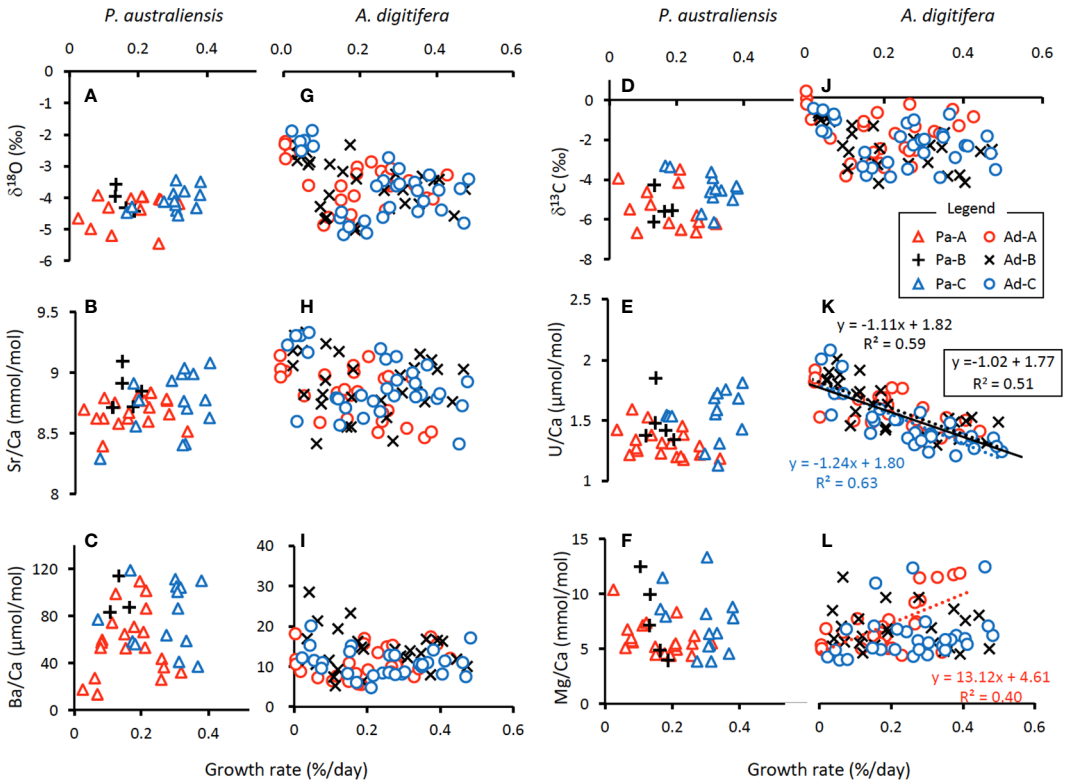

FIGURE 7
Variations in chemical compositions of each colony of *P. australiensis* **(A-F)** and *A. digitifera* **(G-L)** as a function of growth rate. Calibrations are presented only for those with an observed significant relationship ($r > 0.5$, $p < 0.05$). Colored dotted lines represent the observed relationships within a colony, while a black line in **(K)** indicates the relationship observed for data from all three colonies.

in the field. Direct comparisons of the growth rates of different species in the field were difficult because of the different depths and wave energies near the sites where corals dwell, as well as their colony size (Nakamura and Yamasaki, 2005; Pratchett et al., 2015). However, Pratchett et al. (2015) compiled the annual extension rates for 148 coral taxa measured using methods such as direct measurements following tagging or staining. As a result, most *Acropora* corals, including *A. digitifera*, had an annual extension rate greater than 30 mm/yr., whereas that of *Porites* was approximately 10 mm/yr. Although the method how to evaluate coral growth is different between our study and those conducted in the field, the results found in the present experiment seems to roughly reflect actual coral activities occurring in the coral reefs.

There have been many reports that vigorous calcification by scleractinian corals is enabled by their symbiotic relationship with photosynthesizing zooxanthellae, as referred to light enhanced calcification (LEC; reviewed by Gattuso et al., 1999; Inoue et al., 2018). However, the exact mechanism facilitating coral calcification through photosynthesis has been still unknown (reviewed by Davy et al., 2012). Therefore, the relationship between the photosynthetic efficiencies of symbiotic algae represented by *Fv/Fm* and coral growth rate in this experiment was examined. Likely to the growth rate, the *Fv/Fm* showed a colony difference for *P. australiensis* but not for *A. digitifera*, especially during the first half of the experiment (Figure 4). Although the difference in growth rate may be attributed to *Fv/Fm*, as it was higher in *A. digitifera* than in *P. australiensis* throughout the experiment, the growth pattern cannot be simply explained solely by *Fv/Fm*, particularly for *A. digitifera*. For example, the growth rate at 18°C remained the lowest throughout the experiment including the first half, when *Fv/Fm* maintained higher values (Figures 3F, G, 4E, F). Similarly, for *P. australiensis*, the *Fv/Fm* of Pa-A was higher than that of the other colonies, but the growth rate of Pa-A was similar to or lower than that of Pa-C (Figures 3A–D, 4A–C). Cohen et al. (2016) hypothesized that blue light signaling and its animal receptors may influence LEC. This suggests that a direct effect of light, rather than being mediated by the photosynthetic process, as reported previously (Gattuso et al., 1999; Al-Horani et al., 2003), may trigger the LEC. Nevertheless, in the present study, strong positive correlations between the growth rate and *Fv/Fm* were observed in all colonies of *P. australiensis* (Figure 5A). Therefore, photosynthesis appeared to have a predominant effect on skeletal growth, although other mechanisms also control it. Mallon et al. (2022) examined the interspecies relationships between photosynthesis, respiration, and calcification using photosynthesizing calcifiers in the Caribbean, including *A. cervicornis* and *P. astreoides*. Their results showed that calcification rates were linked to energy production at the organismal level and that the species-specific ratios of net calcification to photosynthesis varied with light over a diurnal cycle. This suggests

that the extent of the impact of photosynthesis on skeletal growth differed between the two species.

In fact, although only the growth response to temperature was similar, other patterns, including the average growth rate, colony differences, and relationship with photosynthesis, differed between the two species. This finding indicates that the strategies of skeletal growth would be different between genus *Porites* and *Acropora*. Also this might be attributed to a tolerance against environmental stresses, as the genus *Porites* may potentially have a greater thermal tolerance than *Acropora* (e.g., Afzal et al., 2023). However, in this study, although several nubbins stopped growing at 30°C for the latter half of the experiment for both species, the overall growth rate was higher for *A. digitifera*, even at 30°C (Figure 3). Furthermore, mortality, which was represented by the number of apparent dead nubbins in this study (13 and eight dead nubbins for *P. australiensis* and *A. digitifera*, respectively, at 30°C), was higher in *P. australiensis* despite its thermal tolerance. Xu et al. (2020) noted a higher contribution of heterotrophic predation in the coral hosts of *Porites* than *Acropora*. They also suggested that the trophic status of stress-tolerant *Porites* is more plastic than that of the vulnerable *Acropora*. In the field, *Porites* might be able to switch from photoautotrophy to heterotrophy; however, we did not feed and used filtered seawater during the experiment. This could be a cause of the suppressed growth and high mortality of nubbins of *P. australiensis* at 30°C. In contrast, *Acropora* appear to belong to the autotrophy among trophic strategies (Conti-Jerpe et al., 2020), consistent with the results that mean *Fv/Fm* and growth rate of *A. digitifera* are higher compared to those for *P. australiensis* in this study. When focusing on growth rate and *Fv/Fm* at 30˚C around the middle of the experiment period (Figures 3B, C, G, H, Figures 4B, C, F, G), *Fv/Fm* and growth rate have decreased for *P. australiensis* while high *Fv/Fm* and positive growth rate have been kept for *A. digitifera*. Under such conditions, *Porites* may shift trophic type from auto- to heterotrophic in the natural coral reef conditions.

4.2 Possible causes of variations of each geochemical compositions

Regarding the variations of chemical compositions, since consistent colony differences have not been detected within the same species (Supplementary Table 1), compiled data using those from three colonies per species are used for discussion. Among multiple chemical compositions, excepting for those at 18˚C as many data of *P. australiensis* at 18˚C were absent, in coral skeletons of two species, Sr/Ca, U/Ca and Mg/Ca were not significantly different between them. These geochemical compositions were scattered within the same range, regardless of the differences in absolute growth rate and growth patterns between the two species. This suggests that the basic mechanisms of incorporation of these chemical compositions might be consistent without large species-specific effects. For Ba/Ca, deviations at each temperature were large in all colonies of *P. australiensis*. This result may have been influenced by the tissue parts, as Ba appears to be enriched in the tissue parts (Alibert and Kinsley, 2008). In addition to Ba/Ca, differences in $\delta^{18}O$ and $\delta^{13}C$ between two species were found, as described above, suggesting the possibility of different mechanisms for incorporating these tracers.

4.2.1 $\delta^{18}O$ variations

It is well known that the $\delta^{18}O$ of coral skeletons mainly for massive *Porites* sp. can be a good proxy for sea surface temperature (SST) and salinity, which affect $\delta^{18}O$ in seawater (e.g., Gagan et al., 2000; Cobb et al., 2003; Hayashi et al., 2013; Inoue et al., 2023). In addition, a potential physiological mechanism that explains the variation of $\delta^{18}O$ based on a model of oxygen isotope fractionation in the $CaCO_3$-dissolved inorganic carbonate (DIC)-H_2O system has been proposed (Derviendt et al., 2017; Inoue et al., 2018). In the latter hypotheses, the skeletal $\delta^{18}O$ values of scleractinian corals might be influenced by the hydration reaction of metabolic CO_2 in the calcifying fluid. Since the carbonic anhydrase (CA) enzyme appears to increase the rate of CO_2 hydration in coral tissue (Hopkinson et al., 2015), differences in mean $\delta^{18}O$ between *A. digitifera* and *P. australiensis* might be attributed to variations in physiological mechanisms between the two species. However, clear temperature dependences are found in both species (Figure 6A), suggesting that activities of the CA would be independent to temperature variations.

4.2.2 Sr/Ca variations

Like $\delta^{18}O$, the Sr/Ca ratios of coral skeletons of massive *Porites* sp. has been widely used to reconstruct past SST (e.g., Corrége, 2006; Ramos et al., 2020). In contrast to the variability of $\delta^{18}O$ in seawater, which depends on the balance between evaporation and precipitation, the residence times of both Sr and Ca in seawater are generally long (>10^6 years; Drever, 1988). Then coral Sr/Ca has been considered a robust proxy for only SST. Additionally, Inoue et al. (2018) reported that the Sr/Ca of symbiotic and aposymbiotic polyps were not significantly different, while there was a difference in $\delta^{18}O$ levels between them. Although the kinetic effect on Sr/Ca through the activity of the Ca^{2+}-ATPase pump has also been reported (e.g., Cohen and McConnaughey, 2003), no Sr/Ca variations related to growth and no clear species-specific effects were found in the incorporation of strontium in this study (Figures 7B, H). However, there are relatively large variations in Sr/Ca within the same temperature settings. Given their large deviation within a specific colony (Supplementary Figures 2B, H), this may not be attributed to physiological regulations. Instead, it could be influenced by variations in nano- to micro-scale skeletal architecture as discussed below.

4.2.3 U/Ca variation

The incorporation of uranium into coral aragonite has been suggested to be controlled by SST (Min et al., 1995; Felis et al., 2009) and pH or DIC (Inoue et al., 2011; DeCarlo et al., 2015; Gothmann and Gagnon, 2021). In this study, although temperature dependencies of U/Ca were partially observed for *A. digitifera* (Supplementary Figure 2K), no clear trends as SST proxy were found (Figure 6E). Inoue et al. (2018) demonstrated distinct variations in U/Ca levels between symbiotic and aposymbiotic polyps. Changes in internal DIC and pH due to photosynthesis

have been linked to variations in pH within the calcifying fluid of these polyps. The U/Ca ratios of *A. digitifera* in this study have shown a significant negative correlation with the growth rate (Figure 7K). As coral U/Ca is negatively correlated with pH (Inoue et al., 2011), this trend might reflect variations in the internal pH probably through the photosynthesis. However, despite the differences in growth rate and *Fv/Fm*, there are no differences in the meanU/Ca between *P. australiensis* and *A. digitifera*. This suggests that other mechanisms may be involved in controlling the incorporation of uranium during skeletal growth. To thoroughly investigate the relationship between skeletal growth, internal pH and skeletal U/Ca ratios, additional data on internal pH would be necessary.

4.2.4 $\delta^{13}C$ variation

Although the mechanisms controlling $\delta^{13}C$ variation in coral skeletons are disputed (McConnaughey, 1989; Reynaud-Vaganay et al., 2001; Grottoli, 2002; Suzuki et al., 2003; Omata et al., 2008; Linsley et al., 2019), $\delta^{13}C$ values in biogenic carbonate generally depend on the photosynthetic rate. This is because ^{12}C is preferentially taken up during photosynthesis, and then ^{13}C-enriched DIC within the calcifying fluid is used to precipitate $CaCO_3$ shells or skeletal material. This leads to a positive correlation between carbonate $\delta^{13}C$ values and photosynthetic rate. In fact, the $\delta^{13}C$ values in symbiotic and aposymbiotic polyps showed differences at the control temperature of 27°C. However, the values measured from bleached symbiotic polyps at 31 and 33°C decreased to approach the values obtained from aposymbiotic polyps (Inoue et al., 2018). As mentioned above, since *Fv/Fm* level was higher in *A. digitifera* compared to *P. australiensis*, overall high values of $\delta^{13}C$ of *A. digitifera* may indicate active photosynthesis compared to *P. australiensis* (Figure 6D). However, variation patterns of $\delta^{13}C$ of both the species in response to temperature cannot be explained simply by *Fv/Fm*, suggesting that complex factors including respiration and kinetic effects would affect the isotope fractionation of carbon during the skeletal growth.

4.2.5 Mg/Ca variation

The Mg/Ca ratio in coral skeletons appears to be influenced by biological effects (Fallon et al., 2003; Meibom et al., 2004; Inoue et al., 2018), although it was initially predicted to be a proxy for SST (Mitsuguchi et al., 1996; Watanabe et al., 2001). Although previous studies have indicated that skeletal Mg/Ca ratios are primarily influenced by the skeletal growth rate from a thermodynamic perspective (Inoue et al., 2007; Brahmi et al., 2012), it appears that they are affected by biological processes rather than purely thermodynamic effects. In particular, the distribution of Mg within the coral host appears to be related to the presence of organic matrix (OM), which is an essential precursor for aragonite crystal precipitation (Cuif et al., 2003; Finch and Allison, 2008; Yoshimura et al., 2015). In fact, there are no significant differences in Mg/Ca between symbiotic and aposymbiotic polyps, despite the significant differences in growth rate (Inoue et al., 2018). In this study, no differences in Mg/Ca were observed in *A. digitifera* and *P. australiensis* (Figure 6F), suggesting that some fundamental biological processes involved in the production of OM for aragonite precipitation might be similar between the two species. Furthermore, the secretion of OM does not appear to depend on water temperature, as our study did not find any correlation between temperature and Mg/Ca (Figure 6F).

4.2.6 Ba/Ca variation

The Ba/Ca ratio in coral skeletons has been utilized for reconstructing river runoff and sediment loads (e.g., McCulloch et al., 2003; Ito et al., 2020) because barium is desorbed from fine-grained suspended particles at the estuarine mixing zone (Li and Chan, 1979). The Ba/Ca ratio in corals grown in a reef unaffected by large rivers has been used to identify indications of upwelling, which transports both dissolved seawater and marine biological barium (Alibert and Kinsley, 2008; Spreter et al., 2022). Recently, it has been used to predict the concentrations of dissolved barium in seawater (Kershaw et al., 2023) and the growth rate of aragonite (Mavromatis et al., 2018). Furthermore, there is a report Indicating that light conditions affect the Ba/Ca in coral skeletons (Yamazaki et al., 2021). However, there have been few studies examining the relationship between coral Ba/Ca and water temperature. The results obtained from this study showed very large variations of Ba/Ca, probably due to tissue parts, at the same temperature, especially for *P. australiensis*, indicating the difficulty of using coral Ba/Ca as an SST proxy. However, a negative relationship was found in *A. digitifera* (Figure 6C). Therefore, some caution might be needed for the use of Ba/Ca as environmental proxies, especially when reconstructing the upwelling, as it brings cold seawater together with dissolved barium.

4.3 Assessment of coral geochemical tracers as a temperature proxy

As reported for *Porites* spp. (Reviewed by Thompson, 2022), the $\delta^{18}O$ and Sr/Ca of all colonies of *A. digitifera* also showed clear negative correlations with temperature without consistent growth rate dependences (Figures 6, 7). Regarding the mean temperature dependences of $\delta^{18}O$ and Sr/Ca calculated using all data from three colonies of *P. australiensis* without data at 18°C, the temperature sensitivities of both tracers appeared to be lower compared to published values. Gagan et al. (2012) reported that the $\delta^{18}O$-SST sensitivities for *Porites* ranged from -0.08 to -0.22 ‰/°C. They also discovered that corals with slow growth throughout the tissue layer were less sensitive to changes in SST. The temperature sensitivity of $\delta^{18}O$ of *P. australiensis* in this study was -0.11 ‰/°C, which is applicable to slow-growing corals. Similarly, a broad range of Sr/Ca-SST sensitivities were reported for *Porites* sp., from -0.041 to -0.082 mmol/mol/°C (Gagan et al., 2012). The mean temperature sensitivity of Sr/Ca in this study (-0.040 mmol/mol/°C) was lower than the published values, and it may represent a slow-growing type, same as $\delta^{18}O$. Reynaud et al. (2007) also reported a significant negative correlation as a quadratic function between Sr/Ca of *Acropora* sp. and temperature. In addition, a strong negative

linear correlation between $\delta^{18}O$ and temperature was observed within the temperature range from 22 to 29°C in their study. Similar to *P. australiensis*, the $\delta^{18}O$ and Sr/Ca of *A. digitifera*, in this study, showed relatively lower temperature sensitivities of -0.17 ‰/°C and -0.033 mmol/mol/°C, respectively. For the $\delta^{18}O$ of *Acropora* sp., -0.30 to -0.34 ‰/°C was reported by Reynaud et al. (2007) and Juillet-Leclerc et al. (2014), which is even higher compared to that reported for *Porites* sp. However, a temperature sensitivity calculated using data obtained from the fibers precipitated during the nighttime was -0.19 ‰/°C (Juillet-Leclerc et al., 2018), which is similar to that found in the present study. In addition to $\delta^{18}O$, Juillet-Leclerc et al. (2014) demonstrated a clear Sr/Ca-temperature relationship, with a temperature range 22-29°C, for *Acropora* sp. cultured with different light intensities. Temperature sensitivities differed between high-light and low-light conditions in which higher (-0.061 mmol/mol/°C) and lower (-0.036 mmol/mol/°C) sensitivities were observed for high- and low-light conditions, respectively. In addition, Ross et al. (2019) reported -0.07 mmol/mol/˚C as temperature dependence of Sr/Ca measured from *Acropora* spp. grown under the natural reef conditions. The similarity of $\delta^{18}O$ and Sr/Ca-temperature sensitivities in this study with those obtained from skeletons precipitated under nighttime and low-light conditions suggests that the growth of *A. digitifera* was slower compared to those grown in the field and/or under more high-light conditions. This is consistent with the findings observed from *P. australiensis*. Although Mallon et al. (2022) suggested the importance of considering natural variations in light for all reef metabolism studies, light intensity in this study (120-140 mmol/m^2/s) was relatively low. This light condition would produce low calcification rates for both species, and the temperature sensitivities would differ from those obtained using corals from the field. However, a calibration study using *Isopora* collected from the Heron Island, located at the southern end of the Great Barrier Reef, demonstrated temperature dependences of -0.18 ‰/°C and -0.061 mmol/mol/˚C for $\delta^{18}O$ and Sr/Ca, respectively (Brenner et al., 2017). The former was the same as that found in this study, whereas the latter was close to that reported in a study performed under high light conditions (Juillet-Leclerc et al., 2014). Because the number of studies on calibrations using corals other than *Porites* remains small, we cannot deduce which values of temperature sensitivity are most appropriate. However, the temperature sensitivity of geochemical tracers, especially for the $\delta^{18}O$ of *Acropora*, appears to not significantly differ from that reported for *Porites*, suggesting its potential as a temperature proxy.

Gagan et al. (2012) suggested that in general, new aragonite is deposited in the calyx (within 2 mm of the growth surface), although in some cases calcification occurs throughout the depth of the tissue layer. In terms of calibration, culture experiments for a relatively short period, such as a couple of weeks to months, apparently cannot provide an elaborate analog for corals in the field because tissue parts cover the skeleton. Instead, these experiments can be used to investigate the possibility of a proxy for a specific factor, such as the growth rate, temperature, and/or pCO_2 by changing the parameter(s). Culture experiments, including those of Reynaud et al. (2007) and this study, have demonstrated a high potential for using $\delta^{18}O$ and Sr/Ca of *Acropora* sp. as temperature proxies in addition to those of *Porites*. Specifically, the $\delta^{18}O$ of *A. digitifera* seems to vary consistently as a function of temperature, without the colony dependence and deviations seen in trace elements such as Sr/Ca. The $\delta^{18}O$ variations reported by Reynaud et al. (2007) also showed a strong negative correlation (r^2 = 0.99) with very small deviations at each temperature setting. Furthermore, $\delta^{18}O$ in polyp samples of *A. digitifera* showed negative correlations with the temperature, from 27 to 33˚C, for both symbiotic and aposymbiotic polyps and even for bleached polyps of symbiotic polyps under thermal stress conditions (31 and 33˚C, Inoue et al., 2018). These findings indicate a stable behavior of $\delta^{18}O$ in response to temperature during the growth of coral skeletons, regardless of differences in growth rate, colony size, and/or photosynthesis efficiency. Nevertheless, because $\delta^{18}O$ -temperature sensitivities have differed among studies, as noted above, caution is advised when using the $\delta^{18}O$ of *Acropora* sp. as a temperature proxy. Corals grown in the field or culturing tanks for more than one year, such as in Hayashi et al. (2013), would be most useful in establishing a robust calibration.

In contrast to the $\delta^{18}O$, the Sr/Ca ratios in the nubbins of *A. digitifera* showed large deviations even at the same temperature setting (Figure 6B). Corals have small polyps in living surface and calcify skeletal corallites that are arranged in three-dimensional fans within the corallum with new corallites forming along the apex of the fan (Veron, 1986; Darke and Barnes, 1993). Comparisons of geochemical determinations using *Porites* sp. between the central and margin part of a fan of corallites which precipitated in the same year have revealed that the margin have higher coral Sr/Ca values (Alibert and McCulloch, 1997). Therefore, DeLong et al. (2013) recommended to use optimal sampling path which along the central axis of an actively extending corallite fan to reconstruct SST precisely. In addition, the distribution of magnesium is strongly correlated with the fine-scale structure of the skeleton (Meibom et al., 2004; Holcomb et al., 2009). Because skeletal parts composed of multiple polyps grown on an acrylic plate were used for the measurements in this study, differences in skeletal architecture may produce large deviations in Sr/Ca in addition to Mg/Ca. To test whether deviations in Sr/Ca and Mg/Ca become small when only the axis of corallite fan is measured, the tip of each nubbin, which is assumed to correspond to the apical parts of corallite fan, was shaved, and Sr/Ca and Mg/Ca were measured using ICP-optical emission spectrometer (ICP-OES; Agilent Technology, 720 series) via the same method described in Genda et al. (2022). Consequently, the deviations decreased, particularly for Mg/Ca, but the temperature dependence of Sr/Ca disappeared (Figure 8). Because the samples were not marked with isotope doping or alizarin red in this study (Suzuki et al., 2005; Gagnon et al., 2012), we could not confirm whether the skeletal parts used for this test grew only during the experimental period. However, this result may suggest that the skeletal growth of *A. digitifera* during the experiment in this study progressed along the acrylic plate rather than growing upward. Although the calibration of Sr/Ca-SST, using the Sr/Ca measured on apical part like performed by Ross et al. (2019), cannot be established in this study, it is important to subsample the skeletal parts along a growth axis of a specific

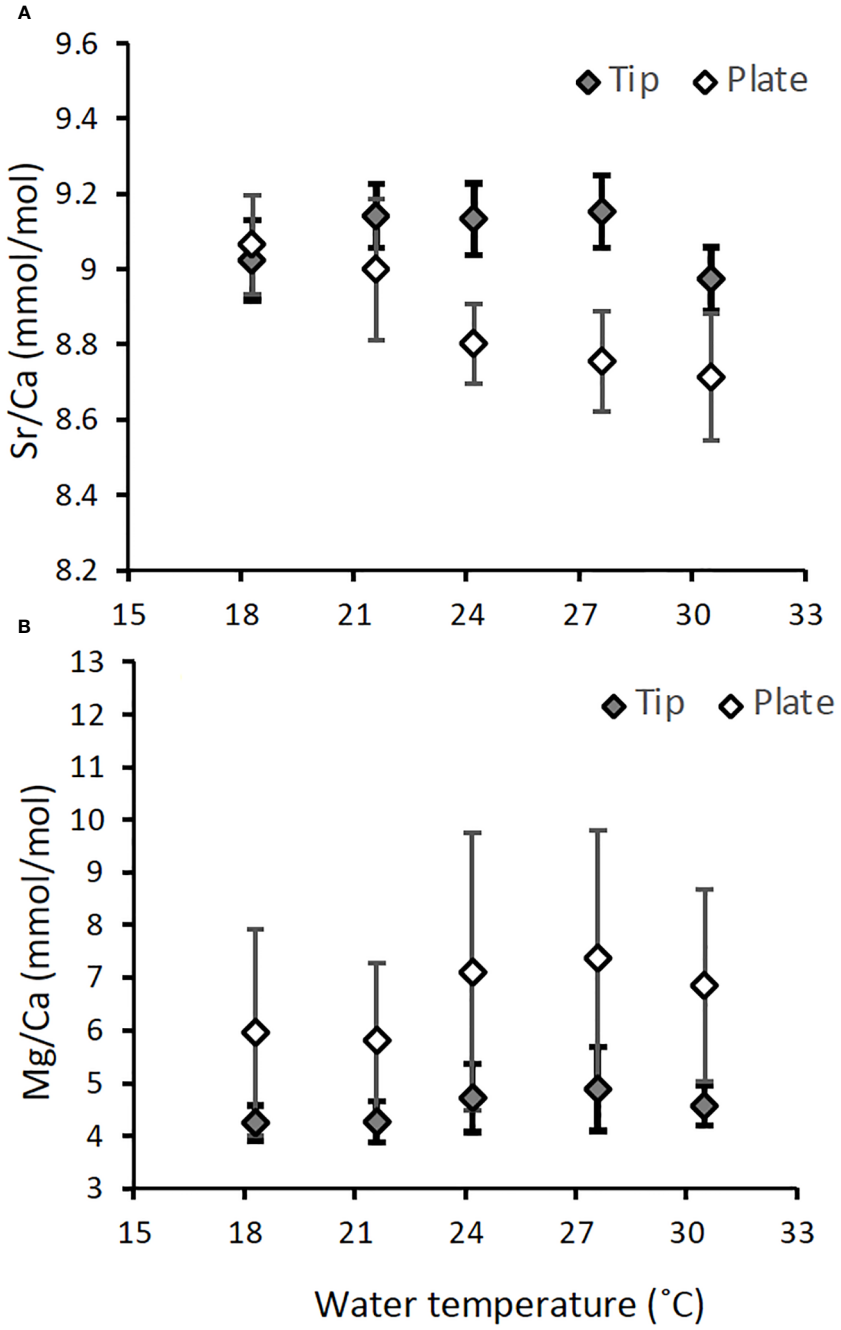

FIGURE 8
Comparison of Sr/Ca **(A)** and Mg/Ca **(B)** contained in skeletal samples collected from skeletons grown on the acrylic plate (white diamond, n = 87 and 80 for Sr/Ca and Mg/Ca, respectively) and the tips of the nubbins (filled diamond, n= 90 and 79 for Sr/Ca and Mg/Ca, respectively) for *A. digitifera*. Results are presented as mean ± 1 sd of the combined data of three colonies.

polyp of *Acropora*, like *Porites* as proposed by DeLong et al. (2013), to ensure the use of precise proxies.

4.3 Implications of biomineralization based on variations of $\delta^{13}C$ and U/Ca

As mentioned above, the systematic difference in $\delta^{13}C$ values between the two species could be explained by the difference in the photosynthesis efficiency, represented by *Fv/Fm*. Although mechanisms of $\delta^{13}C$ variations against temperature for both species were unclear, they were likely mixed with metabolic and kinetic effects on $\delta^{13}C$. For example, lowered $\delta^{13}C$ at 30°C may be attributed to the respiration since it decreased the $\delta^{13}C$ of coral skeletons (Figure 6D, Schoepf et al., 2014). On the other hand, the kinetic effect may have overwhelmed other factors changing $\delta^{13}C$ in coral skeletons at 18˚C, as the growth rate at 18°C was the lowest (McConnaughey, 1989). Accordingly, the relationship between the

$\delta^{18}O$ and $\delta^{13}C$ of *A. digitifera* at the same temperature demonstrated kinetic control, whereas *P. australiensis* did not (Figure 9). Therefore, the $\delta^{13}C$ of *A. digitifera* appears to reflect its photosynthesis, respiration, and growth rate. In contrast, water temperature was the predominant controlling factor for the $\delta^{18}O$ of *A. digitifera*, without a strong growth rate dependence. However, the existence of kinetic effects within a specific temperature should be considered when utilizing the $\delta^{18}O$ of *Acropora* corals in reconstructions of paleo-SST.

Several studies have suggested that the U/Ca ratio in coral skeletons is controlled by pH or DIC within the calcifying space (Inoue et al., 2011; DeCarlo et al., 2015; Inoue et al., 2018; Gothmann and Gagnon, 2021). Additionally, a microsensor-based determination of DIC in the extracellular calcifying medium of *Stylophora pistillata* showed that photosynthesis and respiration exerted a strong influence on chemistry, such as the pH of the calcifying space during light and dark periods (Sevilgen et al., 2019). Although the mean U/Ca values of the two species were not significantly different, a strong growth rate dependence of U/Ca was found only in *A. digitifera* (Figure 7K). Additionally, U/Ca ratios in *A. digitifera* also showed weak to moderate negative correlations with temperature, but those at higher temperature especially at 30°C shifted toward more higher values than expected from the calibration lines (Supplementary Figure 2K). A similar behavior of U/Ca in response to temperature is also found for *P. australiensis* (Figure 6E). Therefore, the U/Ca ratio of *A. digitifera*, and likely *P. australiensis* as well, at 30°C seems to reflect the growth rate, which is associated with fluctuations in pH or DIC. As seawater pH was consistent for all aquariums, the higher shift in U/Ca at 30°C may suggest that the pH of the calcifying space was lower, as U/Ca is negatively correlated to pH, than that of nubbins reared under other temperature settings. Considering the variation pattern of both U/Ca and $\delta^{13}C$ of *A. digitifera* at 30°C, respirations may overwhelm photosynthesis for coral nubbins at 30°C. Consequently, the pH at calcifying space likely decreased owing to the increased respiration rate, which is consistent with the higher shift of U/Ca at 30°C. Additionally, of the decreased pH at the calcifying space may be attributed to the decreased growth rate at 30°C, regardless of the relatively high *Fv/Fm* in *A. digitifera* (Figures 3, 4).

5 Conclusion

Various cultural experiments have been conducted using scleractinian corals, involving variations in parameters such as temperature, light, and/or pCO_2. In this study, a relatively simple culture experiment was conducted, in which only the water temperature was changed for *P. australiensis* and *A. digitifera* for 77 days. In general, the massive *Porites* sp. that grow up to 1-2 m in diameter are primarily located in the Indo-Pacific region. They are often used to reconstruct past SST based on their skeletal $\delta^{18}O$ and Sr/Ca ratios. On the other hand, *Acropora* sp. grow widespread globally and is often found as a fossil, but the potential for its geochemical tracers to serve as temperature proxies has not been thoroughly investigated. Therefore, we examined it using both *P. australiensis* and *A. digitifera*, which are commonly found in the coral reefs around Okinawa, Japan. They were cultured in the same aquaria under identical conditions, with temperatures ranging from 18 to 30°C. We used three colonies of both species to examine genetic differences in growth rate, photosynthetic efficiency (*Fv/Fm*), and variations in geochemical compositions. As a result, the overall growth rates were higher in *A. digitifera* without colony differences, whereas they were lower in *P. australiensis* compared to *A. digitifera* with colony dependences. The responses of skeletal growth to *Fv/Fm* differed between the two species, indicating that the strategies for skeletal growth vary between massive *Porites* and branching *Acropora*. Despite these differences in skeletal growth, the values of Sr/Ca, U/Ca, and Mg/Ca measured in bulk samples, including skeletal parts grown only during the experiment, showed no significant differences. However, $\delta^{18}O$, $\delta^{13}C$, and Ba/Ca exhibited significant differences between the two species. Only Sr/Ca and $\delta^{18}O$ in both species showed significant relationships to temperature, indicating that these tracers of branching *Acropora* have high potential as temperature proxies, as do those of *Porites* sp. Given that kinetic effects are also observed in the $\delta^{18}O$-$\delta^{13}C$

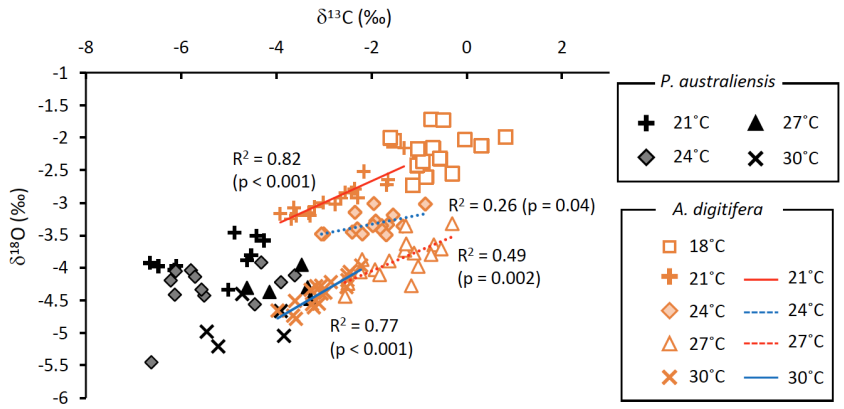

FIGURE 9
Relationships between $\delta^{13}C$ and $\delta^{18}O$ of skeletons grown under the same temperatures for *P. australiensis* (black symbols) and *A. digitifera* (orange symbols). Data are composed of three colonies.

relations at the same temperature setting, it is important to exercise caution when using $\delta^{18}O$ as a temperature proxy. In addition, it is important to sub-sample the apical parts of each polyp to reconstruct environments more precisely.

Data availability statement

The original contributions presented in the study are included in the article/Supplementary Material. Further inquiries can be directed to the corresponding author.

Ethics statement

The manuscript presents research on animals that do not require ethical approval for their study.

Author contributions

SS: Formal analysis, Methodology, Writing – review & editing. MIn: Conceptualization, Funding acquisition, Writing – original draft, Writing – review & editing. YT: Investigation, Methodology, Writing – review & editing. TN: Investigation, Methodology, Writing – review & editing. KS: Investigation, Writing – review & editing. MIk: Formal analysis, Writing – review & editing. AS: Methodology, Writing – review & editing.

Funding

The author(s) declare financial support was received for the research, authorship, and/or publication of this article. This study was supported by the Canon Foundation and JSPS KAKENHI (grant numbers 15H05329 and 26220102). Financial support for the publication of this article was supported by "Initiative for Realizing Diversity in the Research Environment" from MEXT.

Acknowledgments

We thank A. Iguchi and C. Shinzato for their help and advice regarding the culture experiments and discussion. We also thank Y. Yoshinaga and H. Kinjyo for their help and support during the experiments. This study was performed under the cooperative research program of the Center for Advanced Marine Research Core (CMCR) at Kochi University (accession numbers 14B036, 15A033, and 15B029).

Conflict of interest

The authors declare that the research was conducted in the absence of any commercial or financial relationships that could be construed as a potential conflict of interest.

Publisher's note

All claims expressed in this article are solely those of the authors and do not necessarily represent those of their affiliated organizations, or those of the publisher, the editors and the reviewers. Any product that may be evaluated in this article, or claim that may be made by its manufacturer, is not guaranteed or endorsed by the publisher.

Supplementary material

The Supplementary Material for this article can be found online at: https://www.frontiersin.org/articles/10.3389/fmars.2024.1329924/full#supplementary-material

References

Abram, N. J., Wright, N. M., Ellis, B., Dixon, B. C., Wurtzel, J. B., England, M. H., et al. (2020). Coupling Indo-Pacific climate variability over the last millennium. *Nature* 579, 385–392. doi: 10.1038/s41586-020-2084-4

Afzal, M. S., Ikeda, K., Ueno, M., and Nakamura, T. (2023). *Dynamics of coral reef communities in Sekisei Lagoon, Japan, following the severe mass bleaching event of 2016, in the Coral Reefs of Eastern Asia under Anthropogenic Impacts*. Eds. I. Takeuchi and H. Yamashiro (Springer, Cham: Coral Reefs of the World 17), 37–52. doi: 10.1007/978-3-031-27560-9_3

Al-Horani, F. A., Al-Moghrabi, S. M., and De Beer, D. (2003). Mechanism of calcification and its relationship to photosynthesis and respiration in the scleractinian coral *Galaxea fascicularis*. *Mar. Biol.* 142, 419–426. doi: 10.1007/s00227-002-0981-8

Alibert, C., and Kinsley, L. (2008). A 170-year Sr/Ca and Ba/Ca coral record from the Western Pacific warm pool:1. What can we learn from unusual coral records? *J. Geophys. Res.* 113, C04008. doi: 10.1029/2006JC003979

Alibert, C., and McCulloch, M. T. (1997). Strontium/calcium ratios in modern *Porites* corals from the Great Barrier Reef as a proxy for sea surface temperature: Calibration of the thermometer and monitoring of ENSO. *Paleoceanogr* 12, 345–363. doi: 10.1029/97PA00318

Anthony, K. R. N., Kline, D. I., Diaz-Pulido, G., Dove, S., and Hoegh-Guldberg, O. (2008). Ocean acidification causes bleaching and productivity loss in coral reef builders. *Proc. Natl. Acad. Sci.* 105, 17442e17446. doi: 10.1073/pnas.0804478105

Beck, J. W., Edwards, R. L., Ito, E., Taylor, F. W., Récy, J., Rougerie, F., et al. (1992). Sea-surface temperature from coral skeletal strontium/calcium ratios. *Science* 257, 644–647. doi: 10.1126/science.257.5070.644

Brahmi, C., Kopp, C., Domart-Coulon, I., Stolarski, J., and Meibom, A. (2012). Skeletal growth dynamics linked to trace-element composition in the scleractinian coral *Pocillipora damicornis*. Geochim. *Cosmochim. Acta* 99, 146–158. doi: 10.1016/j.gca.2012.09.031

Brenner, L. D., Linsley, B. K., and Potts, D. C. (2017). A modern Sr/Ca-$\delta^{18}O$-sea surface temperature calibration for Isopora corals on the Great Barrier Reef. *Paleoceanography* 32, 182–194. doi: 10.1002/2016PA002973

Cobb, K. M., Charles, C. D., Cheng, H., and Edwards, R. L. (2003). El Niño–Southern oscillation and tropical Pacific climate during the last millennium. *Nature* 424, 271–276. doi: 10.1038/nature01779

Cohen, A., and McConnaughey, T. A. (2003). "Geochemical perspectives on coral mineralization," in *Biomineralization*. Eds. P. M. Dove, J. J. D. Yoreo and S. Weiner (Washington, DC: Mineral. Soc. of Am.), 151–187.

Cohen, I., Dubinsky, Z., and Erez, J. (2016). Light enhanced calcification in hermatypic corals: New insights from light spectral responses. *Front. Mar. Sci.* 2. doi: 10.3389/fmars.2015.00122

Conti-Jerpe, I. E., Thompson, P. D., Wong, C. W. M., Oliveira, N. L., Duprey, N. N., Moynihan, M. A., et al. (2020). Trophic strategies and bleaching resistance in reef-building corals. *Sci. Adv.* 6, eaaz5443. doi: 10.1126/sciadv.aaz5443

Corrége, T. (2006). Sea surface temperature and salinity reconstruction from coral geochemical tracers. *Palaeogeogr. Palaeoclimatol. Palaeoecol.* 232, 408–428. doi: 10.1016/j.palaeo.2005.10.014

Cuif, J. P., Dauphin, Y., Doucet, J., Salome, M., and Susini, J. (2003). XANES mapping of organic sulfate in three scleractinian coral skeletons. *Geochim. Cosmochim. Acta* 67, 75–83. doi: 10.1016/S0016-7037(02)01041-4

Cuny-Guirriec, K., Douville, E., Reynaud, S., Allemand, D., Bordier, L., Canesi, M., et al. (2019). Coral li/mg thermometry: caveats and constraints. *Chem. Geol.* 523, 162–178. doi: 10.1016/j.chemgeo.2019.03.038

Darke, W. M., and Barnes, D. J. (1993). Growth trajectories of corallites and ages of polyps in massive colonies of reef-building corals of the genus *Porites*. *Mar. Biol.* 117, 321–326. doi: 10.1007/BF00345677

Davies, P. S. (1989). Short-term growth measurements of corals using an accurate buoyant weighing technique. *Mar. Biol.* 101, 389–395.

Davy, S. K., Allemand, D., and Weis, V. M. (2012). Cell biology of cnidarian-dinoflagellate symbiosis. *Microbiol. Mol. Biol. Rev.* 76, 229–261. doi: 10.1128/MMBR.05014-11

DeCarlo, T. M., Gaetani, G. A., Cohen, A. L., Foster, G. L., Alpert, A. E., and Stewart, J. A. (2016). Coral sr-U thermometry. *Paleoceanography* 31, 626–638. doi: 10.1002/2015PA002908

DeCarlo, T. M., Gaetani, G. A., Holcomb, M., and Cohen, A. L. (2015). Experimental determination of factors controlling the U/Ca ratio of aragonite precipitated from seawater: implications for interpreting coral skeletons. *Geochim. Cosmochim. Acta* 162, 151–165. doi: 10.1016/j.gca.2015.04.016

DeLong, K. L., Quinn, T. M., Taylor, F. W., Shen, C.-C., and Lin, K. (2013). Improving coral-based paleoclimate reconstructions by replicating 350 years of coral Sr/Ca variation. *Palaeogeogr. Palaeoclimatol. Palaeoecol.* 373, 6–24. doi: 10.1016/j.palaeo.2012.08.019

Devriendt, L. S., Watkins, J. M., and McGregor, H. M. (2017). Oxygen isotope fractionation in the $CaCO_3$-DIC-H_2O system. *Geochim. Cosmochim. Act* 214, 115–142. doi: 10.1016/j.gca.2017.06.022

Drever, J. I. (1988). *The geochemistry of natural waters* Vol. 437 (Englewood Cliffs: Prentice hall).

D'Olivo, J. P., Sinclair, D. J., Rankenburg, K., and McCulloch, M. T. (2018). A universal multi-trace element calibration for reconstructing sea surface temperatures from long-lived porites corals: Removing 'vital-effects. ' *Geochim. Cosmochim. Acta* 239, 109–135. doi: 10.1016/j.gca.2018.07.035

Fallon, S. J., McCulloch, M. T., and Alibert, C. (2003). Examining water temperature proxies in *Porites* corals from the Great Barrier Reef: a cross-shelf comparison. *Coral Reefs* 22, 389–404. doi: 10.1007/s00338-003-0322-5

Felis, T., McGregor, H. V., Linsley, B. K., Tudhope, A. W., Gagan, M. K., Suzuki, A., et al. (2014). Intensification of meridional temperature gradient in the Great Barrier Reef following Glacial Maximum. *Nat. Commun.* 5, 4102. doi: 10.1038/ncomms5102

Felis, T., Suzuki, A., Kuhnert, H., Dima, M., Lohmann, G., and Kawahata, H. (2009). Subtropical coral reveals abrupt earlytwentieth-century freshening in the western North Pacific Ocean. *Geol* 37, 527–530. doi: 10.1130/G25581A.1

Finch, A. A., and Allison, N. (2008). Mg structural state in coral aragonite and implications for the paleoenvironmental proxy. *Geophys. Res. Lett.* 35, L08704. doi: 10.1029/2008GL033543

Fitt, W. K., Gates, R. D., Hoegh-Guldberg, O., Bythell, J. C., Jatkar, A. A., Grottoli, A. G., et al. (2009). Response of two species of Indo-Pacific corals, *Porites cylindrica* and *Stylophora pistillata*, to short-term thermal stress: The host does matter in determines the tolerance of corals to bleaching. *J. Exp. Mar. Biol. Ecol.* 373, 102–110. doi: 10.1016/j.jembe.2009.03.011

Gaetani, G. A., Cohen, A. L., Wang, Z., and Crusius, J. (2011). Rayleigh-based, multi-element coral thermometry: A biomineralization approach for developing climate proxies. *Geochim. Cosmochim. Acta* 75, 1920–1932. doi: 10.1016/j.gca.2011.01.010

Gagan, M. K., Ayliffe, L. K., Beck, J. W., Cole, J. E., Druffel, E. R. M., Dunbar, R. B., et al. (2000). New views of the tropical paleoclimate from corals. *Quat. Sci. Rev.* 19, 45–64. doi: 10.1016/S0277-3791(99)00054-2

Gagan, M. K., Dunbar, G. B., and Suzuki, A. (2012). The effect of skeletal mass accumulation in *Porites* on coral Sr/Ca and $\delta^{18}O$ paleothermometry. *Paleoceanography* 27. doi: 10.1029/2011PA002215

Gagnon, A. C., Adkins, J. F., and Erez, J. (2012). Seawater transport during coral biomineralization. *Earth Planet. Sci. Lett.* 329–330, 150–161. doi: 10.1016/j.epsl.2012.03.005

Gattuso, J. P., Allemand, D., and Frankignoulle, M. (1999). Photosynthesis and calcification at the cellular, organismal, and community levels in coral reefs: A review of interactions and control by carbonate chemistry. *Am. Zool.* 39, 160–183. doi: 10.1093/icb/39.1.160

Genda, A., Ikehara, M., Suzuki, A., Arman, A., and Inoue, M. (2022). Sea surface temperature and salinity in Lombok Strait reconstructed from coral Sr/Ca and δ^{18}–2012. *Front. Clim.* 4. doi: 10.3389/fclim.2022.918273

Goodkin, N. F., Samanta, D., Bolton, A., Ong, M. R., Hoang, P. K., Vo, S. T., et al. (2021). Natural and anthropogenic forcing of multi-decadal-to centennial-scale variability of sea surface temperature in the South China Sea. Paleoceanogr. *Paleoclimatol* 36, e2021. doi: 10.1029/2021PA004233

Gothmann, A. M., and Gagnon, A. C. (2021). The primary controls on U/Ca and minor element proxies in a cold-water coral cultured under decoupled carbonate chemistry conditions. *Geochimica Cosmochimica Acta* 315, 38–60. doi: 10.1016/j.gca.2021.09.020

Grottoli, A. G. (2002). Effect of light and brine shrimp on skeletal $\delta^{13}C$ in the Hawaiian coral Porites compressa: A tank experiment. *Geochim. Cosmochim. Acta* 66, 1955–1967. doi: 10.1016/S0016-7037(01)00901-2

Hammer, Ø., Harper, D. A. T., and Ryan, P. D. (2001). PAST: Paleontological Statistics software package for education and data analysis. *Palaeontol. Electron* 4, 9.

Hayashi, E., Suzuki, A., Nakamura, T., Iwase, A., Ishimura, T., Iguchi, A, et al. (2013). The influence of growth rate on coral climate proxies was tested using multiple colony culture experiments. *Earth Planet. Sci. Lett.* 362, 198–206. doi: 10.1016/j.epsl.2012.11.046

Holcomb, M., Cohen, A. L., Gabitov, R. I., and Hutter, J. L. (2009). The compositional and morphological features of aragonite were experimentally precipitated from seawater and biogenically precipitated from coral. *Geochim. Cosmochim. Acta* 73, 4166–4179. doi: 10.1016/j.gca.2009.04.015

Hopkinson, B. M., Tansik, A. L., and Fitt, W. K. (2015). Internal carbonic anhydrase activity in the tissue of scleractinian corals is sufficient to support proposed roles in photosynthesis and calcification. *J. Exp. Biol.* 218, 2039–2048. doi: 10.1242/jeb.118182

Iguchi, A., Ozaki, S., Nakamura, T., Inoue, M., Tanaka, Y., Suzuki, A., et al. (2012). Effects of acidified seawater on calcification and symbiotic algae in the massive coral *Porites australiensis*. *Mar. Environ. Res.* 73, 32–36. doi: 10.1016/j.marenvres.2011.10.008

Inoue, M., Fukushima, A., Chihara, M., Genda, A., Ikehara, M., Okai, T., et al. (2023). Natural and anthropogenic climate variability signals in a 237-year-long coral record from the Philippines. *Paleoceanogr. Paleoclimatol* 38, e2022PA004540. doi: 10.1029/2022PA004540

Inoue, M., Ishikawa, D., Miyaji, T., Yamazaki, A., Suzuki, A., Yamano, H., et al. (2014). Evaluation of Mn and Fe in coral skeletons (*Porites* spp.) as proxies for sediment loading and the reconstruction of 50 years of land use on Ishigaki Island, Japan. *Coral Reefs.* 33, 363–373. doi: 10.1007/s00338-014-1128-3

Inoue, M., Nakamura, T., Tanaka, Y., Suzuki, A., Yokoyama, Y., Kawahata, H., et al. (2018). The simple role of coral-algal symbiosis in coral calcification is based on multiple geochemical tracers. *Geochim. Cosmochim. Acta* 235, 76–88. doi: 10.1016/j.gca.2018.05.016

Inoue, M., Suwa, R., Suzuki, A., Sakai, K., and Kawahata, H. (2011). Effects of seawater pH on the growth and skeletal U/Ca ratios of *Acropora digitifera* coral polyps. *Geophys. Res. Lett.* 38. doi: 10.1029/2011GL047786

Inoue, M., Suzuki, A., Nohara, M., Hibino, K., and Kawahata, H. (2007). Empirical assessment of coral Sr/Ca and Mg/Ca ratios as climate proxies using colonies grown at different temperatures. *Geophys. Res. Lett.* 34, L1261. doi: 10.1029/2007GL029628

Ito, S., Watanabe, T., Yano, M., and Watanabe, T. K. (2020). Influence of local industrial changes on reef coral calcification. *Sci. Rep.* 10, 7892. doi: 10.1038/s41598-020-64877-6

Jones, R., Giofre, N., Luter, H. M., Neoh, T. L., Fisher, R., and Duckworth, A. R. (2020). Coral response to chronic turbidity. *Sci. Rep.* 10, 4762. doi: 10.1038/s41598-020-61712-w

Juillet-Leclerc, A., Reynaud, S., Dissard, D., Tisserand, G., and Ferrier-Pagès, C. (2014). Light is an active contributor to the vital effects of coral skeleton proxies. *Geochim. Cosmochim. Acta* 140, 671–690. doi: 10.1016/j.gca.2014.05.042

Juillet-Leclerc, A., Rollion-Bard, C., Reynaud, S., and Ferrier-Pagès, C. (2018). A new paradigm for $\delta^{18}O$ in coral skeleton oxygen isotope fractionation response to biological kinetic effects. *Chem. Geol.* 483, 131–140. doi: 10.1016/j.chemgeo.2018.02.035

Kershaw, J. A., Stewart, J. A., Strawson, I., de Carvalho Ferreira, M. L., Robinson, L. F., Hendry, K. R., et al. (2023). Ba/Ca of stylasterid coral skeletons records dissolved seawater barium concentrations. *Chem. Geol.* 622, 121355. doi: 10.1016/j.chemgeo.2023.121355

Lajeunesse, T. C., Thornhill, D. J., Cox, E. F., Stanton, F. G., Fitt, W. K., and Schmidt, G. W. (2004). High diversity and host specificity have been observed among the symbiotic dinoflagellates of reef coral communities in Hawaii. *Coral Reefs.* 23, 596–603. doi: 10.1007/s00338-004-0428-4

Li, Y. H., and Chan, L. H. (1979). Desorption of Ba and 226Ra from river-borne sediments in the Hudson estuary. *Earth Planet. Sci. Lett.* 43, 343–350. doi: 10.1016/0012-821X(79)90089-X

Linsley, B. K., Dunbar, R. B., Dassié, E. P., Tangri, N., Henry, W. C., Logan, D. B., et al. (2019). Coral carbon isotope sensitivity to growth rate and water depth with paleo-sea level implications. *Nat. Commun.* 10, 2056. doi: 10.1038/s41467-019-10054-x

Loya, Y., Sakai, K., Yamazato, K., Nakano, Y., Sambali, H., and van Woesik, R. (2001). Coral bleaching: winners and losers. *Ecol. Lett.* 4, 122–131. doi: 10.1046/j.1461-0248.2001.00203.x

Mallon, J., Cyronak, T. J., Hall, E. R., Banaszak, A. T., Exton, D. A., and Bass, A. M. (2022). Light-driven dynamics between the calcification and production of functionally diverse coral reef calcifiers. *Limnol. Oceanogr.* 67, 434–449. doi: 10.1002/lno.12002

Mavromatis, V., Goetschl, K. E., Grengg, C., Konrad, F., Purgstaller, B., and Dietzel, M. (2018). Barium partitioning in calcite and aragonite as a function of growth rate. *Geochim. Cosmochim. Acta* 237, 65–78. doi: 10.1016/j.gca.2018.06.018

McConnaughey, T. (1989). ^{13}C and 18O isotopic disequilibrium in biological carbonates: I. *Patterns. Geochim. Cosmochim. Acta* 53, 151–162. doi: 10.1016/0016-7037(89)90282-2

McCulloch, M. T., Fallon, S. J., Wyndham, T., Hendy, E. J., Lough, J. M., and Barnes, D. K. (2003). Coral records of increased sediment flux to the inner Great Barrier Reef since European settlement. *Nature* 421, 727–730. doi: 10.1038/nature01361

Meibom, A., Cuif, J. P., Hillion, F., Constantz, B. R., Juillet-Leclerc, A., Dauphin, Y., et al. (2004). Distribution of magnesium in coral skeletons. *Geophys. Res. Lett.* 31, L23306. doi: 10.1029/2004GL021313

Min, G. R., Edwards, R. L., Taylor, F. W., Recy, J., Gallup, C. D., and Beck, J. W. (1995). Annual cycles of U/Ca in coral skeletons and U/Ca thermometry. *Geochim. Cosmochim. Acta* 59, 2025–2042. doi: 10.1016/0016-7037(95)00124-7

Mitsuguchi, T., Matsumoto, E., Abe, O., Uchida, T., and Isdale, P. J. (1996). Mg/Ca thermometry in coral skeletons. *Science* 274, 961–963. doi: 10.1126/science.274.5289.961

Montagna, P., McCulloch, M., Douville, E., López Correa, M., Trotter, J., Rodolfo-Metalpa, R., et al. (2014). Li/Mg systematics in scleractinian corals: Calibration of the thermometer. *Geochim. Cosmochim. Acta* 132, 288–310. doi: 10.1016/j.gca.2014.02.005

Nakamura, T., and Yamasaki, H. (2005). Requirement of water flow for sustainable growth of pocilloporid corals during high-temperature periods. *Mar. pollut. Bull.* 50, 1115–1120. doi: 10.1016/j.marpolbul.2005.06.025

Nakamura, T., van Woesik, R., and Yamasaki, H. (2005). The photoinhibition of photosynthesis is reduced by water flow in the reef-building coral *Acropora digitifera*. *Mar. Ecol. Prog. Ser.* 301, 109–118. doi: 10.3354/meps301109

Okai, T., Suzuki, A., Kawahata, H., Terashima, S., and Imai, N. (2002). Preparation of new geological survey of Japan geochemical reference material: coral JCp-1. *Geostand. Geoanal. Res.* 26, 95–99. doi: 10.1111/j.1751-908X.2002.tb00627.x

Omata, T., Suzuki, A., Sato, T., Minoshima, K., Nomaru, E., Murakami, A., et al. (2008). Effect of photosynthetic light dosage on carbon isotope composition in the coral skeleton: Long-term culture of Porites spp. *J. Geophys. Res.* 113, G02014. doi: 10.1029/2007JG000431

Pelejero, C., Calvo, E., McCulloch, M. T., Marshall, J. F., Gagan, M. K., Lough, J. M., et al. (2005). Pre-industrial to modern interdecadal variability in coral reef pH. *Science* 309, 2204–2207. doi: 10.1126/science.1113692

Pratchett, M. S., Anderson, K. D., Hoogenboom, M. O., Widman, E., Baird, A. H., Pandolfi, J. M., et al. (2015). Spatial, temporal and taxonomic variation in coral growth—implications for the structure and function of coral reef ecosystems. *Oceanogr. Mar. Biol. Annu. Rev.* 53, 215–295. doi: 10.1201/b18733-7

Ram, S., and Erez, J. (2021). The distribution coefficients of major and minor elements in coral skeletons under variable calcium seawater concentrations. *Front. Earth Sci.* 9. doi: 10.3389/feart.2021.657176

Ramos, R. D., Goodkin, N. F., and Fan, T.-Y. (2020). Coral records at the northern edge of the western Pacific warm Pool reveal multiple drivers of sea surface temperature, salinity, and rainfall variability since the end of the Little Ice Age. Paleoceanogr. *Paleoclimatol* 35, e2019 doi: 10.1029/2019PA003826

Reynaud, S., Ferrier-Pagès, C., Meibom, A., Mostefaoui, S., Mortlock, R., Fairbanks, R., et al. (2007). Light and temperature effects on Sr/Ca and Mg/Ca ratios in the scleractinian coral *Acropora* sp. *Geochim. Cosmochim. Acta* 71, 354–362. doi: 10.1016/j.gca.2006.09.009

Reynaud-Vaganay, S., Juillet-Leclerc, A., Jaubert, J., and Gattuso, J. P. (2001). Effect of light on skeletal δ^{13}C and d δ^{18}O, and interaction with photosynthesis, respiration and calcification in two zooxanthellate scleractinian corals. *Palaeogeogr. Palaeoclimatol. Palaeoecol.* 175, 393–404. doi: 10.1016/S0031-0182(01)00382-0

Ross, C. L., DeCarlo, T. M., and McCulloch, M. T. (2019). Calibration of Sr/Ca, Li/Mg and Sr-U paleothermometry in branching and foliose corals. *Paleoceanogr. Paleoclimatol.* 34, 1271–1291. doi: 10.1029/2018PA003426

Schoepf, V., Levas, S. J., Rodrigues, L. J., McBride, M. O., Aschaffenburg, M. D., Matsui, Y., et al. (2014). Kinetic and metabolic isotope effects in coral skeletal carbon isotopes: A re-evaluation using experimental coral bleaching as a case study. *Geochim. Cosmochim. Acta* 146, 164–178. doi: 10.1016/j.gca.2014.09.033

Sevilgen, D. S., Venn, A. A., Hu, M. Y., Tambutté, E., De Beer, D., Planas-Bielsa, V., et al. (2019). Full in *vivo* characterization of carbonate chemistry at the site of calcification in corals. *Sci. Adv.* 5, eaau7447. doi: 10.1126/sciadv.aau7447

Spreter, P. M., Reuter, M., Mertz-Kraus, R., Taylor, O., and Brachert, T. C. (2022). Calcification response of reef corals to seasonal upwelling in the northern Arabian Sea (Masirah Island, Oman). *Biogeosci* 19, 3559–3573. doi: 10.5194/bg-19-3559-2022

Suzuki, A., Gagan, M. K., Fabricius, K., Isdale, P. J., Yukino, I., and Kawahata, H. (2003). Skeletal isotope microprofiles of growth perturbations in Porites corals during the 1997–1998 mass bleaching event. *Coral Reefs* 22, 357–369. doi: 10.1007/s00338-003-0323-4

Suzuki, A., Hibino, K., Iwase, A., and Kawahata, H. (2005). Intercolony variability of skeletal oxygen and carbon isotope signatures of cultured *Porites* corals: Temperature-controlled experiments. *Geochim. Cosmochim. Acta* 69, 4453–4462. doi: 10.1016/j.gca.2005.05.018

Thompson, D. M. (2022). Environmental records from coral skeletons: A decade of novel insights and innovation. *Wiley Interdiscip. Reviews: Climate Change* 13 (1), e745. doi: 10.1002/wcc.745

Veron, J. E. N. (1986). *Corals of Australia and the indo-pacific* (Sydney: Angus & Robertson), 644.

Watanabe, T., Winter, A., and Oba, T. (2001). Seasonal changes in sea surface temperature and salinity during the Little Ice Age in the Caribbean Sea deduced from Mg/Ca and ^{18}O/^{16}O ratios in corals. *Mar. Geol.* 173, 21–35. doi: 10.1016/S0025-3227(00)00166-3

Wei, G., Wang, Z., Ke, T., Liu, Y., Deng, W., Chen, X., et al. (2015). Decadal Variability in seawater pH in the west Pacific: Evidence from coral δ^{11}B records. *J. Geophys. Res.* 120, 7166–7181. doi: 10.1002/2015JC011066

Xu, S., Yu, K., Zhang, Z., Chen, B., Qin, Z., Huang, X., et al. (2020). Intergeneric differences in trophic status of scleractinian corals from Weizhou Island, northern South China Sea: Implication for their different environmental stress tolerance. *J. Geophys. Res.* 124, e2019JG005451. doi: 10.1029/2019JG005451

Yamazaki, A., Yano, M., Harii, S., and Watanabe, T. (2021). Effects of light on the Ba/Ca ratios in coral skeletons. *Chem. Geol.* 559, 119911. doi: 10.1016/j.chemgeo.2020.119911

Yoshimura, T., Tamenori, Y., Takahashi, O., Nguyen, L. T., Hasegawa, H., Iwasaki, N., et al. (2015). Mg coordination in biogenic carbonates constrained by theoretical and experimental XANES. *Earth Planet. Sci. Lett.* 421, 68–74. doi: 10.1016/j.epsl.2015.03.048